HHS Public Access

Author manuscript

Nat Med. Author manuscript; available in PMC 2023 June 26.

Published in final edited form as:

Nat Med. 2023 March ; 29(3): 689–699. doi:10.1038/s41591-022-02202-6.

EPIDURAL STIMULATION OF THE CERVICAL SPINAL CORD FOR POST-STROKE UPPER LIMB PARESIS

Marc P. Powell[1,2,*], **Nikhil Verma**[3,4,*], **Erynn Sorensen**[1,2,5,*], **Erick Carranza**[2,5,6], **Amy Boos**[2,7], **Daryl P. Fields**[1,2], **Souvik Roy**[1,2], **Scott Ensel**[2,5,6], **Beatrice Barra**[2], **Jeffrey Balzer**[1], **Jeff Goldsmith**[8], **Robert M. Friedlander**[1], **George F. Wittenberg**[2,7,9], **Lee E. Fisher**[2,5,6,10], **John W Krakauer**[11,12,13,14], **Peter C. Gerszten**[1], **Elvira Pirondini**[2,5,6,**], **Douglas J Weber**[3,4,15,**], **Marco Capogrosso**[1,2,5,**]

[1]Department of Neurological Surgery, University of Pittsburgh, Pittsburgh, PA, USA

[2]Rehab and Neural Engineering Labs, University of Pittsburgh, Pittsburgh, PA, USA

[3]Department of Mechanical Engineering, Carnegie Mellon University, Pittsburgh, PA, USA

[4]NeuroMechatronics Lab, Carnegie Mellon University, Pittsburgh, PA, USA

[5]Department of Bioengineering, University of Pittsburgh, Pittsburgh, PA, USA

[6]Department of Physical Medicine and Rehabilitation, University of Pittsburgh, Pittsburgh, PA, USA

[7]Department of Neurology, University of Pittsburgh, Pittsburgh, PA, USA

[8]Department of Biostatistics, Columbia University, New York, NY, USA

[9]Veteran Affairs HS, Pittsburgh, PA, USA

[10]Department of Biomedical Engineering Carnegie Mellon University, Pittsburgh, USA

[11]Department of Neurology, Johns Hopkins University, Baltimore, USA

[12]Department of Neuroscience, Johns Hopkins University, Baltimore, USA

[13]Department of Physical Medicine and Rehabilitation, Johns Hopkins University, Baltimore, USA

Correspondence to: Marco Capogrosso, mcapo@pitt.edu.

*These authors contributed equally,

**these authors jointly supervised this work

AUTHORS CONTRIBUTIONS

MC, DW and EP conceived the study. MC, DW and EP secured funding. MC, EP, JK and DW designed the experiments and assessments. MP, DW, NV and ES designed and implemented the stimulation control system, hardware and software framework for the experiments. EC and EP designed and implemented KINARM motor tasks. SE and EP designed and performed MRI-based analyses. AB and GW implemented patient recruitment, eligibility and monitoring and coordinated study management. MC, LF and PG designed the neurosurgical approach. PG, DF and RF implemented and evaluated neurosurgical procedures and participants' clinical management protocols. JB, MP and MC designed and performed intraoperative monitoring protocols. MP, NV, ES, EC, MC, EP, SR, BB, AB and JK performed the experiments. JG designed statistical data analyses. MP, NV, ES, EC and SR analyzed the data. MP, ES, EC and NV created the figures. MC, MP, EP, DW, ES and NV wrote the paper and all authors contributed to its editing.

CODE AVAILABILITY

All software used to produce the figures in this manuscript will be available upon reasonable request to the corresponding author.

COMPETING INTERESTS STATEMENT

MP, DW, MC and PG are founders and shareholders of Reach Neuro Inc. a company developing spinal cord stimulation technologies for stroke. EP has interest in Reach Neuro Inc due to personal relationship with MC. MP, DW, MC, PG, EP, ES, NV and EC are inventors on patents related to this work. All other authors declare no competing interests.

[14]The Santa Fe Institute, Santa Fe, USA

[15]The Neuroscience Institute, Carnegie Mellon University, Pittsburgh, PA, USA

Abstract

Cerebral strokes can disrupt descending commands from motor cortical areas to the spinal cord, which can result in permanent motor deficits of the arm and hand. However, below the lesion, the spinal circuits that control movement remain intact and could be targeted by neurotechnologies to restore movement. Here we report results from two participants in a first-in-human study using electrical stimulation of cervical spinal circuits to facilitate arm and hand motor control in chronic post-stroke hemiparesis (NCT04512690). Participants were implanted for 29 days with two linear leads in the dorsolateral epidural space targeting spinal roots C3 to T1 to increase excitation of arm and hand motoneurons. We found that continuous stimulation through selected contacts improved strength (e.g. grip force +40% SCS01; +108% SCS02), kinematics (e.g. +30% to +40% speed), and functional movements, thereby enabling participants to perform movements that they could not perform without SCS. Both participants retained some of these improvements even without stimulation and no serious adverse events were reported. While we cannot conclusively evaluate safety and efficacy from two participants, our data provides promising, albeit preliminary, evidence that SCS could be an assistive as well as a restorative approach for upper limb recovery after stroke.

Globally, 1 in 4 people will suffer from a stroke[1]. Of these people, nearly three quarters will exhibit lasting deficits in motor control of their arm and hand[2] that cause enormous personal and societal impact[3]. These motor deficits persist partly due to the failure of current neurorehabilitation approaches to significantly reduce upper limb impairement[4].

Patients with chronic stroke exhibit a stereotypical motor syndrome of the upper limb that can be decomposed into independently quantifiable deficits[5]: loss of strength, reduced dexterity, intrusion of aberrant synergies, and disorders of muscle tone. This *paresis* phenotype emerges from damage to the cortico-spinal tract (CST), which disrupts connections between the cortex and the cervical spinal circuits controlling arm and hand movements[5–7].

Given that in most cases damage to the CST is incomplete, we posited that voluntary motor control could be restored by amplifying the capacity of the residual CST. Specifically, we hypothesized that modulating the excitability of intact sub-lesional spinal circuits would increase their responsiveness to remaining CST neurons, thereby restoring the ability of these supra-spinal inputs to drive movement. A century of research has shown that primary sensory afferent neurons in the dorsal roots provide a pathway for influencing spinal circuit excitability[8–15]. Furthermore, we and others have demonstrated that epidural spinal cord stimulation (SCS), a clinically approved technology, can be utilized to directly recruit these afferents[16–18], thus providing a means to test our CST augmentation hypothesis in humans with chronic stroke.

Clinical support for SCS comes from studies exploring its use in the recovery of locomotion after spinal cord injury[19–25] (SCI). While most of these studies focused on

quantifying the cyclic patterns of movement involved in walking[21,23,26], several groups reported that SCS enabled people with complete leg paralysis to produce voluntary single-joint movements[19,20,22]. This movement facilitation was immediate and required SCS to remain on; providing an assistive effect[19,20,24]. Importantly, this SCS-related assistive effect is distinct from the involuntary movements elicited by technologies such as functional electrical stimulation (FES)[27,28]. Rather than directly producing movement, SCS facilitates the ability of residual propriospinal and supraspinal inputs to activate spinal motoneurons, thereby enabling volitional movement[20,29–31]. Moreover, when the assistive effect of SCS was combined with prolonged behavioral training, it promoted long-lasting recovery of voluntary leg motor function even in the absence of stimulation; thus demonstrating a therapeutic effect[22,25].

Despite these encouraging findings for leg motor recovery, epidural stimulation of the cervical spinal cord to target upper limb recovery has been largely unexplored (see these animal studies[15,16,32,33] and a single pilot in humans[34]). In addition to paucity of evidence, application of SCS to the post-stroke upper-limb motor syndrome is hindered by disease-specific scientific and technical challenges. Dexterous control of the arm and hand relies more heavily on cortico-spinal input[35] than does control of locomotion[11,36], so for the same degree of residual CST, the degree of spinal circuit potentiation required may be greater. Moreover, the physiology of post-stroke motor deficits is different from SCI and therefore the response to SCS may be qualitatively different. For example, pharmacological treatments are more effective in treating spasticity after SCI than spasticity after stroke[37]. From a technical perspective, the cervical enlargement is significantly longer and larger than the lumbosacral spinal cord, which makes current clinical paddle leads insufficient to cover all the segments innervating upper limb muscles[16]. Here, building upon our work in monkeys[15,16] we sought to overcome these challenges and tested the efficacy of cervical SCS to restore upper limb motor deficits in humans with post-stroke arm and hand paresis. Specifically, we designed a neurosurgical approach that implants two staggered linear leads on the lateral aspect of the cervical cord to target each dorsal root innervating arm and hand muscles at their entry into the spinal cord[15,16,38].To determine whether continuous SCS could improve cortico-spinal control, we devised a battery of scientific and clinical assessments to quantify the assistive effects of SCS on strength, dexterity, synergies, and spasticity.

RESULTS

Study design and experimental setup

In this study we report results from the first two participants of an ongoing study (NCT04512690) that seeks to obtain feasibility and preliminary data on the effects of cervical SCS on motor control in people with chronic post-stroke upper limb paresis using continuous trains of stimulation pulses delivered at a fixed amplitude and rate through selected contacts (Figure 1). SCS01, Caucasian female, 31 years old, suffered a right thalamic hemorrhagic stroke secondary to a cavernous malformation 9 years prior to participation in the study. SCS02, Caucasian female, 47 years old, suffered a right ischemic middle cerebral artery stroke secondary to a right carotid dissection resulting in

a large MCA territory infarct 3 years prior to participation in the study. Informed consent was given by all study participants prior to enrollment. SCS01's lesion was localized to the internal capsule, midbrain, and pons, while SCS02's lesion was larger, affecting the corona radiata of the right hemisphere (Figure 1d, Extended Data Figure 1). In both cases, the extensive damage to the CST led to chronic upper limb impairment. We performed a tractography analysis using high-definition fiber tracking (HDFT) to compare the integrity of CST axons between the lesioned and healthy hemispheres. (Extended Data Figure 1). Relative white matter integrity was then determined by comparing Fractional anisotropy (FA) of the lesioned hemisphere to the non-lesioned hemisphere. We obtained FAS=0.17 for SCS01 and FAS=0.35 for SCS02 (FAS=0 no impairment, see methods), which indicated significant unilateral damage to the CST in both participants. This was reflected in pre-study Fugl-Meyer motor assessments of 35/66 (SCS01) and 15/66 (SCS02), indicative of moderate and severe impairment respectively.

This pilot study was designed to quantify the immediate, assistive effects of continuous SCS on post-stroke motor deficits, including muscle weakness, impaired dexterity of arm and finger movements, intrusion of aberrant flexor synergies and abnormal tone. Based on previous work in SCI, we expected any immediate benefit to reverse once SCS was turned off[15,20–22,24]. In this pilot trial, we did not incorporate activity-based training exercises into the protocol and instead focused on measuring immediate improvements attributable to the direct effects of SCS in facilitating motor function in the arm and hand. Testing began four days after implantation of the SCS leads and continued for four weeks, during which the subjects participated in assessments sessions five times per week, approximately 4 hours per day. After 29 days the percutaneous leads were removed. In each session, we evaluated function with and without stimulation that we delivered continuously through a custom-built microcontroller-based system connected via percutaneous access to the SCS leads (Extended Data Figure 2).

Cervical SCS achieves segment-level muscle recruitment

Clinical SCS leads are intended to be placed along the midline to broadly stimulate dorsal columns and block pain signals[39]. We have shown previously in monkeys and humans that more selective recruitment of primary afferent fibers in the cervical dorsal rootlets can be achieved by positioning the clinical SCS leads laterally, near the dorsal root entry zone[15,16,38]. These primary afferents innervate motoneuron pools according to a well-defined rostro-caudal somatotopy[40], and we predicted that stimulating specific nerve roots would lead to excitation of the corresponding motoneurons[40] (Figure 1c). Consequently, we hypothesized that selective stimulation of rostral roots (e.g. C4) would facilitate muscle activation in the upper arm, while stimulation of the caudal roots (e.g. C8–T1) would target distal muscles including the forearm and hand[16]. Therefore, we designed a surgical approach to implant two linear electrodes mediolaterally spanning the dorsal roots C4 to T1 (Figure 1b). During implantation, we guided surgical placement with neurophysiological intraoperative monitoring[22] and verified that reflex-mediated muscle responses could be obtained reliably across all muscles of the arm and hand. Intra-operative data showed that SCS followed a clear rostro-caudal segmental specificity in both participants (Figure 1d and Extended Data Figure 3). Monopolar stimulation of rostral contacts induced activity

in the deltoids and trapezius while caudal contacts recruited intrinsic hand muscles (Figure 1**f** and **h** and Extended Data Figure 3). To verify that stimulation responses resulted from afferent-mediated recruitment of the motoneurons, and not by directly recruiting ventral roots, we stimulated through the same contact at different frequencies (1.1, 2, 5, 10, and 20 Hz). Reflex mediated responses are well known to show frequency-dependent suppression phenomena[10,16]. The peak-to-peak amplitude of evoked muscle activity was reduced significantly in a frequency dependent manner confirming that motor neuron activation was occurring trans-synaptically (Extended Data Figure 4). Repeated X-rays showed minimal rostro-caudal displacement of the leads from the implant (Extended Data Figure 1) which did not affect functional performance and we utilized the same contact configurations from week 2 (when they were finalized) to week 4 (Figure 2). Stimulation intensity was adjusted daily to levels that enabled volitional movements but did not produce any passive joint movement or torques at rest[19–21].

In summary, we showed that accurate placement of clinical leads over the dorsolateral cervical spinal cord produces selective muscle activation according to pre-existing myotomal maps and that stimulation activates motor activity through sensory afferents in the dorsal roots.

Arm and hand strength immediately improved with SCS on

To determine whether SCS would lead to an increase in strength, we asked participants to apply their maximum force during isometric flexion and extension at single arm joints. Forces were applied to a robotic platform which measured joint torque (HUMAC NORM) (Figure 3 g). We compared torques produced with and without continuous SCS targeting muscles of the tested joint (Figure 3). We found that SCS01 consistently increased strength for shoulder and elbow flexion and extension; mean torques at the elbow more than doubled when SCS was provided (Day 9: 9.8 vs 22.0 Nm; Day 23: 11.6 vs 24.6 Nm) (Figure 3a, c,e). Instead, at the wrist, SCS01 was unable to perform the wrist extension task with forces detectable by our system even with SCS. We could, however, measure consistent improvement in wrist flexion torques (Figure 3d). As an example of the functional relevance of these improvements, we show a video in which SCS01 can raise her arm above her head during SCS (Video 1). In SCS01, we tested multiple stimulation frequencies (20, 40 and 60Hz) during elbow flexion and extension isometric tests and found that 60Hz yielded maximal torques (Extended Data Figure 5a). The severity of SCS02's impairment hindered consistent assessment of some joints. Specifically, she could produce detectable torques during shoulder flexion and extension and demonstrated significant improvements in elbow flexion torque (Figure 3a,c,e) similar to those observed in SCS01 (40% average increase), but we were not able to measure elbow extension or wrist torques either with or without SCS.

We also tested isometric grip strength using a hand-held dynamometer (Figure 3f). SCS led to a 40% increase in SCS01 and a 108% increase in SCS02 suggesting that SCS can potentiate both arm and hand function. This result was particularly striking for SCS02 who had near complete left-hand paralysis and was unable to consistently produce detectable hand grip forces (as measured with a hand dynamometer) without SCS. Additionally, on the

first day of testing, SCS01, for the first time in the 9 years since her stroke, immediately reacquired the capacity to fully and volitionally open her hand (Video 1). We also compared the root mean square values of EMG signals measured from the anterior deltoid, biceps, and triceps during elbow extension (SCS01) and elbow flexion (SCS02). EMG was substantially higher with stimulation than without for these muscles in both participants (>100% increase Figure 3a,b) indicating that SCS potentiates the participant's ability to recruit muscles.

Since participants were always aware that stimulation was active due to SCS induced paresthesias[38], we performed sham trials in which non-optimal stimulation was delivered without participant knowledge to control for motivation bias. In these sham trials, we selected electrodes that preferentially activated muscle groups that were antagonistic to the movement performed (e.g. electrode 8R facilitated extension and 2R facilitated flexion). SCS01 still experienced paresthesia over the shoulder and arm during stimulation and was unable to distinguish optimal from sub-optimal configurations. As expected, while even antagonist stimulation led to some increase in strength (+19% extension using 2R, 2.2mA, 60Hz; 7C, 3.6mA, 60Hz and +16% flexion using 8R, 2.4mA, 60Hz; 7C, 3.6mA, 60Hz), the most significant improvements in strength occurred only when SCS was optimized for the intended movement (agonistic stimulation; +82% extension using 8R, 2.4mA, 60Hz; 7C, 3.6mA, 60Hz and +25% flexion using 2R, 2.2mA, 60Hz; 7C, 3.6mA, 60Hz) (Extended Data Figure 6 a). In summary, we showed that SCS led to immediate and substantial improvements in strength and muscle activity of the arm and hand when optimal contacts were used.

SCS improved arm motor control during planar reaching

In addition to strength, we evaluated the benefit of SCS on arm dexterity and muscle synergies. For this, both participants performed planar reach and pull tasks using a robotic platform (KINARM) that supported the weight of their arm (Figure 4a). Importantly, these reaching tasks were performed in the horizontal plane to dissociate the effects of shoulder weakness and compensatory movements from the capacity of participants to extend their arm towards a target[41].

SCS01 was asked to reach towards different targets positioned to maximize active elbow extension since this was particularly difficult for the participant due to the intrusion of flexor synergies. During continuous stimulation, SCS01 was able to successfully reach all targets; whereas, without stimulation, she was never able to reach the central target (Figure 4b). Movements to targets that she could consistently reach with and without stimulation, were significantly smoother with stimulation active (Figure 4c; 34% (left target) and 47% (right target) fewer velocity peaks). Similarly, speed (Figure 4c; 41% (left target), 37% (right target) faster), trajectory, variability, and max distance reached, were all improved with stimulation compared to controls (Extended Data Figure 5b).

Due to the severity of SCS02's impairment and to reduce frustration, she performed a simpler task in which she was instructed to reach the furthest of three horizontal lines spaced at 10 cm intervals (Figure 4d). Despite the simpler concept, the task assessed the same reaching and pulling arm kinematics in the same space as SCS01. Without stimulation, SCS02 was never able to reach the farthest line, but with stimulation on she was able to

reach it on every trial due to the facilitation of elbow extension. This was reflected in the elbow excursion angle, which increased 23 degrees with stimulation (Figure 4e). The maximum distance reached was 7.8 cm greater and total movement time was 37% faster with stimulation, (Figure 4e). Like SCS01, her movements also became smoother during stimulation (20% fewer velocity peaks Extended Data Figure 5c), and her trajectory variance and total path length also significantly improved (Extended Data Figure 5c). Arm extension kinematics and elbow angle were strongly modulated by stimulation frequency in SCS02 showing peak performances at 100Hz (Extended Data Figure 5a).

We hypothesized that the improvements in reaching function were attributable to facilitation of elbow muscle activity and changes in flexion and extension synergies. To test this, we inspected EMG activity and extracted muscle flexor and extensor synergies associated with the extension and flexion movement phases using dimensionality reduction (Figure 5, see supplementary information). Without stimulation, muscle activity was very low at the elbow muscles and very high at the shoulder muscles, likely indicating a compensatory strategy dominated by shoulder muscles and allowing the elbow to extend passively during the reach. This was reflected in the strength of the components of each synergy that showed a greater contribution of shoulder muscles in both participants(Figure 5d,f,i). Instead, with stimulation, the contribution of elbow muscles increased and became dominant in both synergies which suggests a reduction of compensatory shoulder movements(Figure 5d,f,i).

To test if stimulation specificity was necessary for optimal motor control, we performed a sham-controlled task in which frequency and amplitude matched non-optimal stimulation was delivered without participant knowledge in the center out task (sham: 4R, 4.4mA, 50Hz; 7R, 4.8mA, 100Hz; 8C, 4.6mA, 50Hz vs optimized: 1C, 4.4mA, 50Hz; 1R, 4.6mA, 50Hz; 5C, 4.8mA, 100Hz). Extended Data Figure 6b–e shows the dramatic impact of incorrect stimulation configuration on SCS02's task performance. Specifically, during sham-stimulation, arm kinematics suffered dramatically and her performance worsened, even compared to her ability with stimulation off, significantly affecting her ability to reach designated targets. Instead, with optimal stimulation she reached all targets 100% of the time.

In summary, despite differences in deficits and task difficulty, we showed that SCS targeting dorsal roots at specific cervical segments immediately improved dexterity and enabled both participants to perform smooth and effective arm movements enabling full elbow extension, improving elbow extension and flexion synergies and reducing compensatory shoulder activity.

Functional benefits of SCS

Finally, we sought to determine whether these improvements in strength and control translated to functional movements and improved performance during activities of daily living (ADL) (Figure 6). For this, we personalized tasks according to impairment level and chose ADLs based on observations of early-study improvements and subjects' rehabilitation goals. We first evaluated the ability of SCS01 to perform 3D reaching movements. We asked SCS01 to reach as fast as she could towards 6 targets placed on two different horizontal planes that required both planar and upward reaching movements against gravity.

Continuous SCS enabled her to reach targets faster, approximately reducing, by half, the time required to complete the 6 target circuit (Figure 6f). We also asked SCS01 to perform a classic manipulation task: the box and blocks task, in which she was instructed to move small cubic objects from one side of a box to the other by grasping and lifting them over a barrier. With stimulation on, she consistently performed better and, on day 17 post-implant, she more than doubled the number of blocks transferred when stimulation was off. Her score increased from 6 blocks without stimulation to 14 blocks during stimulation (Figure 6e, Video 2). We also assessed function with the Action Research Arm Test[42] (ARAT). SCS01's pre-study baseline score was 31/57. At the end of the study, we administered the test both with and without stimulation, with resulting scores of 45/57 and 36/57 respectively; representing a 14 point improvement while SCS was active. Finally, we increased the complexity of the tasks by presenting activities of daily living that required high skill and dexterity such as drawing a spiral, reaching for and lifting a soup can, eating with a fork, and opening a lock. SCS increased her overall dexterity, allowing her to produce smoother and more consistent drawings (Figure 6a). Stimulation also enabled simultaneous reaching, forearm supination and grasp allowing SCS01 to reach, grasp and lift a soup can. Without stimulation, forearm pronation and supination were not possible (Figure 6b, Video 3). SCS also enabled fine motor skills such as opening a lock and manipulating utensils to eat independently (Figure 6 c, Video 4); tasks that she had been unable to perform for 9 years.

Since SCS02 was unable to sustain the weight of her arm against gravity, we adapted the 3D reaching task using a clinically approved actuated exoskeleton robot (Hocoma Armeo Power) to provide titrated assistance during the task (50% arm weight support). We endeavored to keep the movements as similar as possible to those performed by SCS01 to allow for comparison by having the subject collect virtual objects from a room and place them on a target (Figure 6g). With stimulation, SCS02 was significantly more efficient at the task and managed to consistently reach towards more targets than without stimulation across three sessions (Figure 6g). We then asked her to perform a skilled motor task where she had to remove a hollow cylinder from a wooden dowel and slip it over another. With SCS she was not only able to grasp and lift the metal cylinder, but also to place it on the adjacent dowel without any weight support (Figure 6d and Video 5). Without SCS she could not complete any of the steps required for this task. These results from the first two participants in our pilot study show that the assistive effects of SCS may lead to significant improvements in functional performances and activities of daily living.

Tone, spasticity, and lasting effects on motor control

To ensure that increased excitation to the spinal cord via SCS did not exacerbate spasticity or other muscle tone dysfunctions, we measured the Modified Ashworth Scale on each day of testing. To minimize daily assessment duration, we limited joints tested for each participant to those with MAS>1 prior to the study. However, elbow and digit flexion, shoulder external and internal rotation, and shoulder abduction were tested in both subjects, for consistency, regardless of prior history. Over the course of four weeks, we found that SCS did not lead to any worsening nor amelioration in MAS scores (Figure 6i and Extended Data Table 1). Since this pilot was designed to study the assistive rather than the therapeutic effects of SCS, participants did not receive concomitant physical or occupational therapy over the four

weeks. We thus did not expect to observe sustained improvements when SCS was turned off. Nevertheless, when we compared the participants' pre- and post-study Fugl-Meyer scores, SCS01 improved from 35 points at enrollment to 47 points, and SCS02 from 15 points to 18 points. These scores decreased by 1 point at a 4 week follow up visit. (Figure 6h and Extended Data Table 2).

Safety and tolerability of the stimulation

Concerning preliminary safety data, no serious adverse events were reported. SCS01 experienced phlebitis several days after the explant procedure at the end of the study that was resolved with oral antibiotics and was not related to the use of stimulation to the spinal cord. Moreover, the two participants did not report increased rigidity nor painful sensations during SCS. In fact, both patients described the stimulation as a "feeling of power in the arms" or a feeling of "being able to control my arm as if I know what I should do to move it".

DISCUSSION

In this study we report preliminary evidence from two participants showing that continuous SCS targeting cervical dorsal roots could immediately improve upper limb strength, motor control, and function in two humans with moderate to severe post-stroke hemiparesis. This assistive effect is lost when SCS is turned off. However, both participants showed some lasting improvements in motor function by the fourth and final week of the study that were retained even without stimulation. While we cannot conclude on safety and efficacy from two participants, here we discuss the first results obtained in humans on the effects of SCS on post-stroke upper limb hemiparesis.

Although SCS for spinal cord injury (SCI) has recently generated considerable excitement[21–23], anecdotal reports of the beneficial motor effects of SCS in people with SCI, multiple sclerosis, cerebral palsy and even stroke date back more than 40 years[43,44]. Unfortunately, a lack of understanding of the mechanisms of SCS led to considerable variability in implant location, which affected the size and consistency of the observed effects. We now know that SCS engages spinal motoneurons via recruitment of primary afferents, providing excitatory input to motoneurons and interneurons directly connected to these afferents[16–18,29,30]. Thus, it could be hypothesized that by raising the membrane potential of spinal neurons, SCS increases responsiveness to residual cortical inputs and immediately improves voluntary motor control[16,19,31,45]. We define this as the "assistive effect" of SCS. By implanting epidural electrodes over the lateral aspect of the cervical spinal cord, we focused this assistive effect on the arm and hand motor pools most needed for each participant[15,16]. Our data shows that SCS had broad assistive effects on motor control, but we did not assess individuated finger control, which is highly CST-dependent. Nevertheless, we did observe improved dexterity in functional hand tasks; particularly in SCS01. Notably, Video 4 shows SCS01 performing a pinch grasp grab a fork during SCS. This suggests that SCS is tapping into residual CST function. We argue that the large effect sizes we measured were possible because, unlike in SCI, the stroke lesion spares cervical spinal circuits and usually some supraspinal pathways. Indeed, studies of cervical SCS in

SCI have not shown the magnitude of immediate assistive effects at the arm and hand as those that we report here post-stroke[34,46].

Despite large differences between the two subjects in terms of severity, age and time since the stroke, during SCS, both subjects showed a significant improvement in strength (Figure 3), arm kinematics (Figure 4) and functional task performance (Figure 6) compared to their baselines without SCS. However, clinical adoption of SCS for stroke will require the application of simple and standardized parameter optimization protocols. Additionally, here we focused on the immediate assistive effects of SCS with temporary implants, future studies should focus on demonstrating long-term safety and efficacy of a fully implanted SCS system combined with protocolled upper-limb rehabilitation in larger, randomized, controlled studies.

The lateral epidural placement of SCS leads enabled selective targeting of specific dorsal roots which allowed us to use simple yet personalized continuous stimulation protocols. Our surgical approach simplified the personalized parameter tuning by leveraging clear somatotopic organization of the cervical spinal cord. Final configurations were selected during the first 2 weeks following procedures similar to works in SCI[47]. While non-invasive alternatives to SCS are being investigated in SCI[46] our results depended on fine tuning of stimulation parameters at particular contacts, which would not be possible with the limited specificity of transcutaneous SCS[48]. We believe that the simplicity and robustness of our protocol could facilitate translation to the clinic. Indeed, implantation and programming procedures are similar to routine applications of SCS for refractory pain[49].

The most important limitation of our study is the low number of subjects which hinders definitive conclusions on safety or efficacy. Other limitations include the absence of a protocolled upper limb behavioral intervention and the short duration of the study (4 weeks) that may have reduced the amount of recovery that subjects could obtain.

Here we placed an emphasis on quantifying the immediate assistive effects of SCS. In contrast, almost all rehabilitative stroke studies concern recovery after the intervention is over[5,50,51] which makes comparison with literature difficult. That said, although our two participants received no protocolled training, we observed some motor recovery that, for SCS01, was above Minimally Clinical Important Differences (MCID) for the Fugl-Meyer score (+12 FM points; MCID: +7.25). Given the short duration of our study compared to similar works in SCI[22,52] we did not expect to observe restorative effects. Therefore, we believe that our results are a preliminary but promising indication that, by combining SCS with protocolled upper-limb rehabilitation, future studies may lead to higher improvements and promote a true post-stroke restorative effect[45]. This restorative avenue is especially exciting considering the advent of new and more effective impairment-focused behavioral interventions for stroke[5,53,54] that could be combined with SCS into an effective therapy for post-stroke hemiparesis.

Methods

In addition to those reported here, detailed methods on surgical procedures, EMG analysis and stimulation control software can be found in the Supplementary Material.

Trial and Subject information

All experimental protocols were approved by the University of Pittsburgh Institutional Review Board (Protocol STUDY19090210) under an abbreviated IDE. The study protocol is published on ClinicalTrial.gov number NCT04512690. Two female subjects (aged 31 and 47) participated in the study. Both subjects participated in every experiment. Some procedures were modified depending on specific subject deficits, such cases are indicated where appropriate. All subjects provided informed consent according to the procedure approved by the Institutional Review Board of the University of Pittsburgh and subjects were compensated for each day of the trial as well as for travel and lodging during the study period.

Inclusion criteria—Subjects between 21–70 years of age who had suffered from an ischemic or hemorrhagic stroke more than 6 months prior to the start of the study were eligible for participation. All subjects had hemiparesis affecting their upper limb and had a pre-study FM-UE score between 7 and 45. Prior to the study, participants were screened via a medical evaluation. Candidates with severe co-morbidities, previously implanted medical devices, claustrophobia, or who were pregnant, or breastfeeding were excluded from the study. Subjects were not receiving any anti-spasticity, anti-epileptic, or anti-coagulation medications for the duration of the study period.

Study design and data reported—The goal of this exploratory clinical trial is to obtain preliminary evidence of safety and efficacy of Spinal Cord Stimulation (SCS) to improve motor control in people with chronic post-stroke upper-limb hemiparesis. The study is designed as a single-group, open-label, prospective study in which we expect to enroll and retain up to 10 participants with chronic stroke. Given the pilot nature of the study, to minimize safety risks, SCS leads are implanted for a maximum period of 29 days, after which the electrodes are explanted. We designed our primary and secondary outcomes to primarily assess safety and obtain preliminary clinical and scientific evidence of both assistive and long-term effects of SCS.

Briefly, after screening and pre-study baselines, subjects are implanted with clinical SCS leads. Starting from day 4 post-implant, subjects undergo scientific sessions 5 times per week, 4 hours per day, for a total of 19 sessions until explant day. Tasks and measurements during the first 5 to 7 sessions are focused on identifying optimal stimulation configurations that are then maintained for the remaining sessions.

A detailed description of primary and secondary outcomes can be found in Supplementary Information Table 1 as well as on ClinicalTrials.gov NCT04512690.

Briefly, primary outcomes are focused on reporting serious adverse events and assessing pain/discomfort. Specifically, we consider the trial to be successful if there are no serious

adverse events related to the use of the stimulation. We then ask subjects to report and rate, if present, any pain or discomfort that arises from the stimulation with the goal of understanding if intensities required for motor effects are pain/discomfort-free. Secondary outcomes are geared towards scientific and preliminary efficacy goals. In terms of clinical efficacy, we quantify immediate improvements in strength by measuring isometric forces with and without SCS one per week. We rate motor deficits by assessing the Fugle-Meyer evaluation, ARAT assessment pre-study and on the last day of implant, and spasticity via Modified Ashworth Scale daily. We then evaluate function by measuring kinematics of the arm and hand during 2D and 3D reaching and grasping tasks. Finally, we perform a battery of imaging and electrophysiology testing to assess excitability and plasticity of spinal circuits pre-, during and post-study. Below we detail the methods for each of the measurements reported in this trial that are part of the secondary outcome assessments. In this manuscript we reported preliminary results from the first two participants of all the primary outcomes and all the secondary outcomes except those that require additional data on more participants to obtain meaningful analyses, such as imaging and electrophysiology outcomes.

Subject information—In this work, we report results from the first 2 subjects participating in our trial, both of whom were caucasian females. SCS01 (31 years) had a right thalamic hemorrhagic stroke secondary to a cavernous malformation 9 years prior to participation in the study. Her interim history involved several bleeding events with eventual ablation of the malformation with gamma knife radiosurgery. At the time of her participation in our trial, her post stroke residual was a left-sided spastic hemiparesis for which she was receiving botulinum injections in her biceps, brachioradialis, and pronator teres. Botulinum treatments were suspended starting 6 months prior to the study period and continuing through the end of the study. In the years between her initial infarct and participation, she also underwent a C5–6 anterior cervical discectomy and fusion to treat cervical stenosis as well as a flexor tendon lengthening surgery due to spasticity and suffered arm and wrist fractures in her affected arm. For SCS01, we included in this work, analysis of 138 isometric force test repetitions at multiple joints (54 stim off and 84 stim on) and 36 planar reaches (18 with SCS and 18 without SCS). We also report the results of simulated activities of daily living and other motor tasks that were performed at least 1 session per week (see Figure 6). Because of technical and subject availability reasons we could not perform Transcranial Magnetic Stimulation (TMS) tests prior to the study to obtain Motor Evoked Potential (MEP) maps on SCS01.

SCS02 (47 years) had a right ischemic middle cerebral artery stroke secondary to a right carotid dissection resulting in a large MCA territory infarct 3 years prior to participation in the study. Her post stroke residual at the time of participation was a left-sided spastic hemiparesis complicated by a left wrist flexion contracture despite treatment with splinting. For SCS02, we included in this work, analysis of 42 isometric force tests repetitions at multiple joints (21 stim off and 21 stim on) and 57 planar reaches (38 with SCS and 19 without SCS) that were obtained across multiple days during the study. We also report the results of simulated activities of daily living and other motor tasks that were performed at least 1 session per week (see Figure 6). TMS measurements obtained over 9 locations and

11 muscles confirmed that SCS02 was MEP negative (e.g. no MEP present in any of the muscles of the paretic arm)

Safety

We recorded all adverse events and reported them to the Data Safety and Monitoring Board and to the IRB to determine whether these would be related to the delivery of electrical stimulation to the spinal cord. Both subjects successfully completed the protocol with no serious adverse events. SCS01 experienced phlebitis several days after the explant procedure at the end of the study that was resolved with oral antibiotics. The DSMB and IRB determined that this adverse event was not serious and not related to the delivery of SCS to the cervical spinal cord.

Medical imaging

X-ray Imaging—X-ray images were acquired at weekly timepoints in both axial and sagittal views to ensure the stability of lead position.

Lesion Segmentation—MRI was acquired using a 3-T Prisma System (Siemens) using a 64-channel head and neck coil. A T1-weighted structural image was captured using a magnetization-prepared rapid gradient echo (MPRAGE) sequence (TR = 2300 ms; TE = 2.9 ms; FoV = 256 × 256 mm^2; 192 slices, slice thickness = 1.0 mm, in-plane resolution = 1.0 × 1.0 mm). Lesion segmentation was performed manually for each slice of the sequence using the MRIcron image viewer (NITRC) and the resulting region of interest (ROI) was smoothed on all planes using a gaussian smoothing kernel with a full-width at half-maximum of 2mm. MRIcro_GL (NITRC) was used to visualize and export the resulting segmented overlays.

High definition fiber tracking (HDFT)—The same 3-T MRI scanner was configured to use a diffusion spectrum imaging scheme to capture a total of 257 diffusion samples. The maximum b-value used was 4000 s/mm^2 and the in-plane resolution and slice thicknesses were 2 mm. The accuracy of b-table orientation was examined by comparing fiber orientations with those of a population-averaged template[55].

The diffusion data were reconstructed in the MNI space using q-space diffeomorphic reconstruction[56] to obtain the spin distribution function[57]. A diffusion sampling length ratio of 1.25 was used. The output resolution in diffeomorphic reconstruction was 2 mm isotropic. The restricted diffusion was quantified using restricted diffusion imaging[58]. The tensor metrics were calculated and a deterministic fiber tracking algorithm[59] was used to reconstruct the cortico-spinal tract fibers. A tractography atlas[55] was used to map left and right cortico-spinal tracts with a distance tolerance of 16 mm. For the fiber tracking, we used: an anisotropy threshold of 0.035, an angular threshold of 50 degrees, and a step size of 1 mm. Tracks with lengths shorter than 10 mm or longer than 200 mm were discarded. A total of 1,000,000 seeds were placed. Topology-informed pruning[60] was applied to thetudy tractography with 16 iterations to remove false connections. We then calculated the mean fractional anisotropy (FA) values for left and right cortico-spinal tract and the percentage of asymmetry was computed using Stinear's formula:

$$Asymmetry = \frac{FA_H - FA_L}{FA_H + FA_L}$$

Where FA_L is the mean FA value of the CST in the lesioned hemisphere and FA_H is the mean FA value of CST in the intact hemisphere.

Efficacy Assessments: Single joint isometric torque

Maximum isometric strength was measured for the shoulder, elbow, and wrist joints (when possible) using a robotic torque dynamometer (HUMAC NORM, CSMi). To measure torque, the robot's manipulandum was positioned and held at a fixed angle and the subject was asked to apply their maximum force while flexing or extending the joint under test for a sustained period of 5 seconds followed by a 10 to 15 second break. This procedure was repeated 5 times to complete a set. For each joint, the system was configured such that the joint was at a nominal and comfortable angle and so that it was aligned with the manipulandum's center of rotation. To isolate single joint function, the participants were constrained with tight straps at the shoulders as well as additional straps and bracing specific to each joint configuration of the HUMAC NORM. For example, while testing elbow strength, the upper arm and elbow were stabilized against the back of the chair while holding the manipulandum at a 90 degree angle. This ensured minimal shifting. Additionally, while testing wrist strength, the forearm was strapped to the robot's joint stabilization attachment. The HUMAC NORM's suggested configurations were used, when possible, but SCS02 was unable to support the weight of her arm and so was placed in a seated position to measure elbow and shoulder torques instead of the suggested supine position. In addition, a splint was used to secure SCS02's hand to the manipulandum to assist her in holding the handle securely and a counterweight was used where appropriate to offset the mass of the manipulandum and allow for more sensitive measurements. The maximum torque value within each repetition was considered for analysis.

Grip force was measured using a hand dynamometer. Participants were asked to hold the dynamometer and apply their maximum grasping force for five seconds. Before every repetition and after the participant's impaired hand was around the dynamometer, the device was zeroed out to ensure baseline grip force at rest was zero. Each measurement comprised the highest force produced on each of 3 attempts and data were combined across days to assemble enough data for statistical comparison.

Efficacy Assessments: clinical impairment scales

Fugl-Meyer—The Fugl-Meyer Upper-Extremity assessment is a standardized evaluation of upper limb motor control and sensory function[61]. It includes 7 categories of assessments including passive and active range of motion, joint pain, proprioception, and tactile sensation. In total, there are 126 possible points. However, all scores reported in this manuscript correspond to the "Motor Function" sub-score which has a maximum value of 66. A trained medical professional conducted and scored the exam at 4 different timepoints: pre-study, mid-study (approximately 2 weeks after implant), end-of-study (4 weeks), and post-study (1 month after explant).

ARAT—The Action Research Arm Test (ARAT) is another assessment of upper limb motor function that focuses on object interaction and manipulation. It comprises 4 categories including grasp, pinch, grip, and gross movement[42]. Scores can range from 0–57 with 57 representing the highest functional performance[62]. A trained medical professional evaluated SCS01's ARAT performance both before the study, and at the end of the study. While SCS02's score was recorded at the pre-study timepoint, she did not consent to perform the test again at the end-of-study because of fatigue hence these data points are not available for SCS02.

Modified Ashworth Scale—To ensure that SCS was not exacerbating joint spasticity, we performed the Modified Ashworth Scale (MAS) each session day at the beginning of the session. In order to minimize daily assessment duration, we largely limited the joints tested for each participant to those with spasticity prior to the study. However, elbow and digit flexion, shoulder external and internal rotation, and shoulder abduction were tested in both subjects, for consistency, regardless of prior history. This assessment involves passive manipulation of each joint, and ranking spasticity levels from 0–4 (0 being no spasticity). A trained medical professional performed and scored the assessment each day. Here we report both a full breakdown of all joint scores measured on each day for both subjects as well as a "summary score". The summary score was taken to be the average score across all joints for each day.

Functional assessments: Planar reach and pull kinematics

To evaluate upper limb motor control during directed reach and pull movements, we used a robotic augmented reality exoskeleton system (KINARM, BKIN Technologies). Participants were secured in a modified wheelchair and their arms were suspended in the exoskeleton to remove the effects of gravity. The platform displayed virtual targets onto a dichroic augmented reality display in front of the subject that allowed them to visualize their hand position relative to the virtual graphics. The robot's motorized joints permitted the application of a mechanical load to the subject's movements.

Center Out Task—For this task, the participants were asked to reach from a central starting position to one of 3 targets displayed using the AR display, then return to the starting position. On each trial the starting position was displayed, and the robot moved the subject's arm into position, locking it in place. Next the target was presented, and the exoskeleton was unlocked. An audio cue was played after a randomized 100 to 700 ms delay indicating that the subject could begin their movement. The participant was given 10 (SCS01) or 15 (SCS02) seconds to complete each trial. A target was considered acquired when the subject's index finger was within a 0.5 cm radius of the target center for 500 ms. An audio cue indicated the end of the reach phase. If the subject was unable to reach the target, the robot returned the arm to the starting position and the next target was presented. If the trial was successful, the subject's finger was positioned in the center of the target in preparation for the pull phase and locked in place. After a 500 ms delay, the arm was unlocked followed by a final audio cue after another 100–700 ms delay indicating the start of the pull phase, and the subject was required to return their hand to the starting position.

In some trials, a load of $-30\ \frac{Ns}{m^2}$ was applied isotropically to the movement using the exoskeleton to increase the task difficulty. Each target was presented 6 times in random order (unless otherwise noted). For each subject, appropriate targets were selected based on their individual range of motion.

The following metrics were calculated for each trajectory to compare kinematic quality. Trajectory smoothness was calculated as the number of peaks in the velocity profile for both the reach and pull phases. We also measured the total time of the combined reach and pull phases. Total path length was calculated and normalized to the Euclidean distance between the starting position and the target; more efficient movements had a lower value. Finally, the variance of each trajectory was calculated as the mean deviation of the actual trajectory from the mean trajectory calculated across all 5 repetitions of the movement.

Open-Ended Reaching Task—The subject was presented with 3 equally spaced horizontal lines (approximately 15, 25, and 30 cm away from the participant) and was asked to reach from a starting position to the furthest line they could. In this way we assessed how far the subject could reach in an open-ended manner.

During each task, the participant started with their hand as close to their body as they could (maximum elbow flexion). After a verbal cue, they began their movement with the goal of passing the farthest line possible. Once the subject indicated that they had reached their maximum distance, another verbal cue indicated that they should return to their initial position. Task events were manually labeled during the trial by the experimenter. Each set comprised 5 repetitions.

As in the center-out task, a set of metrics was calculated for each trajectory; reach and pull phases were considered separately. Movement duration was calculated as the time it took from the beginning of each phase for the subject to cross the second horizontal line (25 cm) during reach and the first horizontal line during pull (15 cm). Maximum distance was measured as the axial distance between the point closest to the subject and the point furthest from the subject in each phase. Range of motion of the elbow during the task was considered as the angle difference between the most acute and most obtuse elbow angles achieved during each phase. As a metric of smoothness, the number of peaks in the elbow angle velocity profile was counted. Total path length measured the total length of the trajectory from the starting point to the second line (25 cm; reach phase) or from the end position to the first line (15 cm; pull phase) and was normalized by the phase duration. Finally, as a measure of variance, we calculated the distribution of each trajectory timepoint from the mean trajectory. A distribution skewed towards the left indicated that more samples were close to the mean trajectory, whereas a distribution with values towards the right indicated large deviations from the mean trajectory and therefore more variance.

Functional assessments: 3D reaching

Fast reaching task—The participant was presented with 6 targets, all axially equidistant from the subject, but at varying heights and lateral positions. The 3 “lower” targets were at table surface height and the 3 “upper” targets were raised to require shoulder flexion beyond

90 degrees. There was a left, center, and right target at each height. A 7th position was placed directly in front of the subject and was used as a "home" position. Starting with their arm outside the working area, the subject was asked to first touch the home position then touch each of the 6 targets, returning to the home position after each target. For this task, we asked the subject to perform the sequence as fast as possible. The total time it took to reach all 6 targets was recorded.

Robotic 3D reaching task—As an alternative to the fast-reaching task, we used an exoskeleton robot (ARMEO POWER, Hocoma) to assist 3D movements when the subject was unable to lift their arm against the force of gravity (SCS02). This robotic system provides motorized support at each joint of the arm and measures kinematic variables in real time allowing for a subject's real-world movements to be displayed in a virtual video game environment. For this task, objects were presented within a virtual room and the subject was asked to reach toward each object and move it to a different position within the room (ARMEO POWER cleanup game). The robot was configured to provide 50% weight support and assist movements at the "Low Support" setting. Game difficulty was set to "Easy". Each game lasted 3 minutes and the goal was to move as many objects as possible within the time limit. The score was then recorded based on the number of objects successfully moved.

Box and Blocks—When possible, we also evaluated the subject's performance in the "Box and Blocks" task. This is a standardized assessment in which a participant must grasp one small block at a time from one side of a box, lift it over a divider, and drop the block in the other half of the box. The total number of blocks moved from one side to the other within 1 minute was the subject's score.

Functional assessments: Activities of Daily Living

We chose ADLs after an initial assessment phase based on subject ability and preferences. In some instances, we chose tasks that emulate everyday activities that participants had identified as being difficult to perform prior to the study; but that they wished to try after having experienced the stimulation. Since ADLs were customized for each participant, we did not evaluate pre-study performance for these tasks.

Drawing a spiral—We asked the subject to draw a spiral shape using a marker on a plain piece of white printer paper taped down to a table. The goal of the task was to make the curves as smooth as possible and attempt not to overlap each of the concentric rings. The subject was allowed to comfortably position the pen in their hand using their unaffected hand before starting to draw.

Object manipulation—We placed a full, sealed can of soup on a table in front of the participant. The subject was asked to grasp the object from the side, requiring them to supinate their forearm, lift the can, and place it at an adjacent target. This task evaluated the subject's ability to reach, grasp, lift, and release a moderately heavy object. Here, the subject was not allowed to use their unaffected arm to assist in grasping the object.

In an alternative object manipulation task, we asked the subject to hold a wooden plank with vertical dowels (similar to a tower of Hanoi toy) on their lap using their unaffected hand. We

then placed a metal cylinder over one of the dowels. The subject was required to grasp the cylinder, lift it off of the first dowel, align it and place it onto a second dowel, and release the cylinder. An experimenter helped to position the hand on the cylinder before the start of the trial. All other movements were performed by the subject entirely on their own.

Lock opening—As a measure of hand dexterity, we positioned a wooden panel with a shackle-style key-actuated lock on a table in front of the subject, who was asked simply to open the lock using their affected limb. To do this task, the participant was required to grasp and stabilize the lock with one hand (e.g. the unaffected hand), use a pinch grip to grasp the key with the other hand (e.g. the affected hand), and supinate the forearm to twist the key and unlock the lock. The subject then removed the lock from its latch on the wooden panel, replaced it by realigning the shank with the latch, and relocked the lock by aligning and pressing the shank back into the body.

Self-feeding—The subject was presented with small bite sized portions of food on a plate and a plastic fork. They were tasked with first picking up the fork from a table, using it to secure a piece of food, and perform the complex movement of orienting the food toward their mouth in preparation to eat it. Here, the subject was required to initiate picking up the fork with their affected hand but was allowed to reposition it using their unaffected hand before attempting to pick up the food.

EMG Analysis

Isometric contraction (root mean square analysis)—During isometric contractions, EMG was acquired from appropriate muscles using wireless sensors as described above. Empirically, we observed that deltoid EMG signals contained stimulation artifacts during trials where stimulation was active due to the proximity of deltoid muscles to the stimulating electrodes. We removed these artifacts by blanking the signal coinciding with stimulation pulses. All signals were bandpass filtered (25–300 Hz, 5^{th} order Butterworth digital filter) and the root mean square (rms) value was calculated from the filtered data over the full duration of each trial for statistical analysis.

Planar reaching (muscle synergy analysis)—Coordinated movements such as reaching and pulling require the timed co-activation of appropriate muscles to produce accurate and controlled limb motion. We measured which muscles were simultaneously active during planar reaching movements by calculating muscle synergies using non-negative matrix factorization (NNMF), a dimensionality reduction technique[63].

EMG pre-processing was different for SCS01 and SCS02 due to large amplitude stimulation artifacts present in SCS02's EMG data that were not present for SCS01. For SCS01, stimulation artifact was removed by blanking and the resulting data were bandpass filtered (20–500 Hz, 5^{th} order Butterworth digital filter). For SCS02, EMG were first bandpass filtered using a narrower pass band (10–200 Hz, 5^{th} order Butterworth, digital filter) to remove high frequency components of the stimulation artifact. Notch filters (5^{th} order Butterworth) at 50, 100, and 150 Hz were then used to remove low frequency harmonics of the stimulation artifact. The resulting signals from both subjects were rectified, low-pass

filtered (5 Hz, 5th order Butterworth digital filter), and normalized to the maximum EMG value recorded from that muscle over the whole day. Processed EMG was extracted from the reach and pull phases of each movement. Muscle synergies were identified using NNMF.

NNMF decomposes the EMG signals into a synergy activation matrix using the temporal correlation between the activity of individual muscles[63]. The result is a set of one-dimensional timeseries signals for each muscle synergy identified. Each synergy in-turn comprises contributions from multiple muscles as described by a synergy vector. We implemented NNMF with two factors which were selected by observing the point-of-inflection in the residuals vs. number of synergies curve[64]. For each phase of the movement (reach and pull), the primary synergy for that movement was identified as the one that most positively correlated (increased) with the movement. All repetitions of the movement were used to perform the dimensionality reduction. Finally, the contributions of deltoid and elbow muscles were quantified and compared using the primary synergy's synergy vector.

Statistics

Bootstrapping—All statistical comparisons of means presented in this manuscript were performed using the bootstrap method, a non-parametric approach which makes no distributional assumptions on the observed data. Instead, bootstrapping uses resampling to construct empirical confidence intervals for quantities of interest. For each comparison (e.g. comparing stimulation on vs stimulation off for shoulder torque in SCS01, shown in Figure 3c), we construct bootstrap samples by drawing a sample with replacement from observed measurements, while preserving the number of measurements in each condition. We construct 10,000 bootstrap samples and, for each, calculate the difference in means of the resampled data. A 95% confidence interval for the difference in means is obtained by identifying the 2.5th and 97.5th quantiles for the resulting values. The null hypothesis of no difference in the mean was rejected if 0 was not included in the 95% confidence interval. If more than one comparison was being performed at once, we used a Bonferroni correction by dividing this alpha value by the number of pairwise comparisons being performed. Bootstrap statistical analysis was only performed when at least 5 data points were obtained.

Comparison of distributions—Statistical comparison of distributions was done using a two-sample Kolmogorov-Smirnov (KS) non-parametric test using MATLAB. Again, an alpha value of 0.05 was used. Here, we used this test to compare the variability of kinematic trajectories during 2D planar reaching (the open-ended reaching task). The deviations of each trajectory from the mean trajectory were used to build a distribution of deviations. The resulting distributions for two conditions (stimulation off and stimulation on) could then be compared using the KS test.

Extended Data

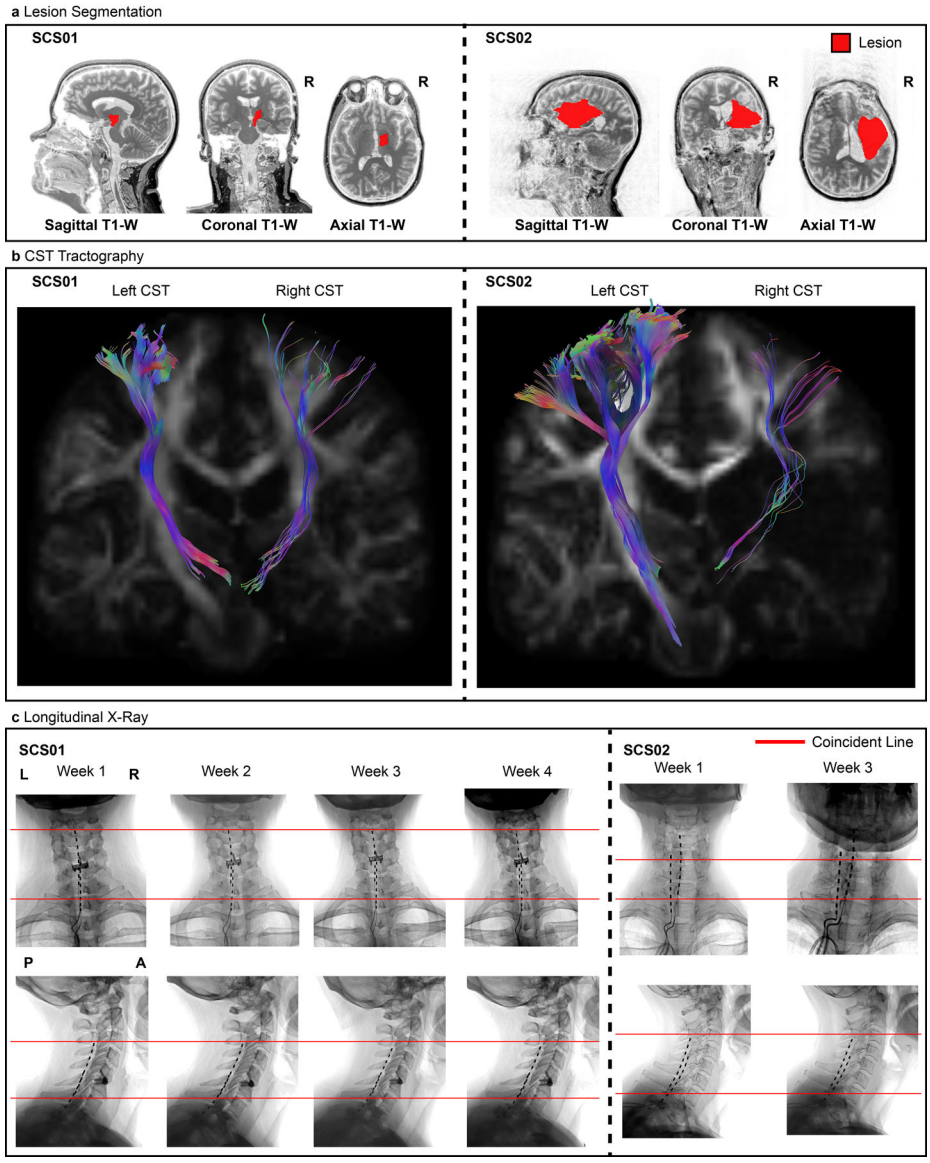

Extended Data Figure 1 |. Lesion characterization and Lead position over time.
(a) sagittal, coronal, and axial T1- weighted MRI 2D projections for SCS01 and SCS02. The segmented lesion is shown in red for both participants. R indicates the Right hemisphere. **(b)** High-definition fiber tracking of the corticospinal tract (CST) for SCS01 and SCS2. Colored fibers represent estimated CTS axons from the affected (right) and unaffected (left) hemisphere. Significant reduction in number of tracked fibers in the right hemisphere is clear in both participants in consequence of the stroke. **(c)** Repeated X-rays for SCS01 (left) and SCS02 (right) showing the position of the spinal leads. The red lines mark the same anatomical location across the X-rays to facilitate interpretation. Minimal displacement occurred after initial implantation.

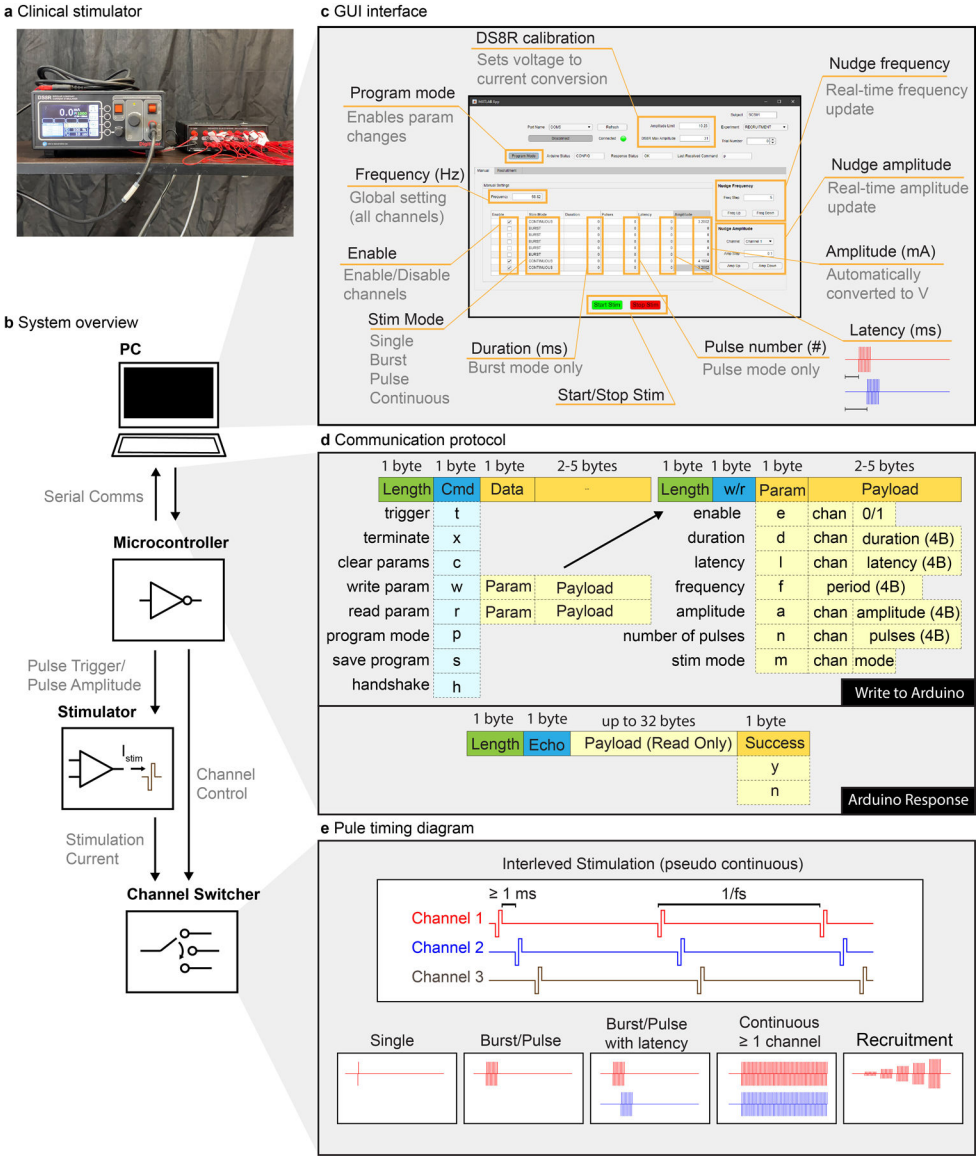

Extended Data Figure 2 |. SCS parameters set using a custom-built controller.

(a) An image of the stimulator (DS8R, left) and 1-to-8 channel multiplexer (D188, right) used to deliver stimulation pulses. **(b)** An overview of the control scheme used to deliver patterns of stimulation. A PC running a **(c)** MATLAB based GUI communicated with a microcontroller using a custom **(d)** communication protocol over a virtual serial port. The microcontroller's firmware delivered pulse triggers and amplitude control signals to the stimulator as well as an 8 bit parallel channel selection signal to the multiplexer in order to control pulse timing, amplitude, and output channel. Current was delivered from the stimulator through the multiplexer and ultimately to the selected electrode on the implanted spinal array. **(c)** The GUI interface allowed for configuring all stimulation parameters including active channels, stimulation frequency, pulse train duration (or continuous), pulse train latency, and stimulation amplitude for each active channel. Once configured, stimulation was initiated or terminated via the software interface. The software also allowed

for rapid changes in either global stimulation frequency (nudge frequency) or channel amplitude (nudge amplitude). **(d)** A custom command protocol layer was developed on top of a UART serial interface to enable communication between the GUI and microcontroller. Each packet from the master (PC) to the slave (microcontroller) comprised a 1 byte packet length, 1 byte command, and 0–6 bytes of payload. A payload comprised a 1 byte parameter (to be read or written), a 1 byte channel number (when appropriate), and the value to be written (when 'write' command was used). Microcontroller response packets comprised a 1 byte packet length, 1 byte command echo, 0–32 bytes of payload (used to return parameter values during 'read' command), and a 1 byte success flag. **(e)** The microcontroller firmware allowed for pseudo-synchronous stimulation across multiple channels by interleaving pulses on all active channels. A delay of at least 1 ms between each pulse allowed enough time for the multiplexer to fully switch channels. The same pattern of pulses was delivered every period as defined by the stimulation frequency. Each channel could also be configured to deliver a single pulse, a pulse train with finite duration and/or latency, continuous stimulation, or a 'recruitment curve' in which the amplitude was gradually increased for successive pulse trains of specified length.

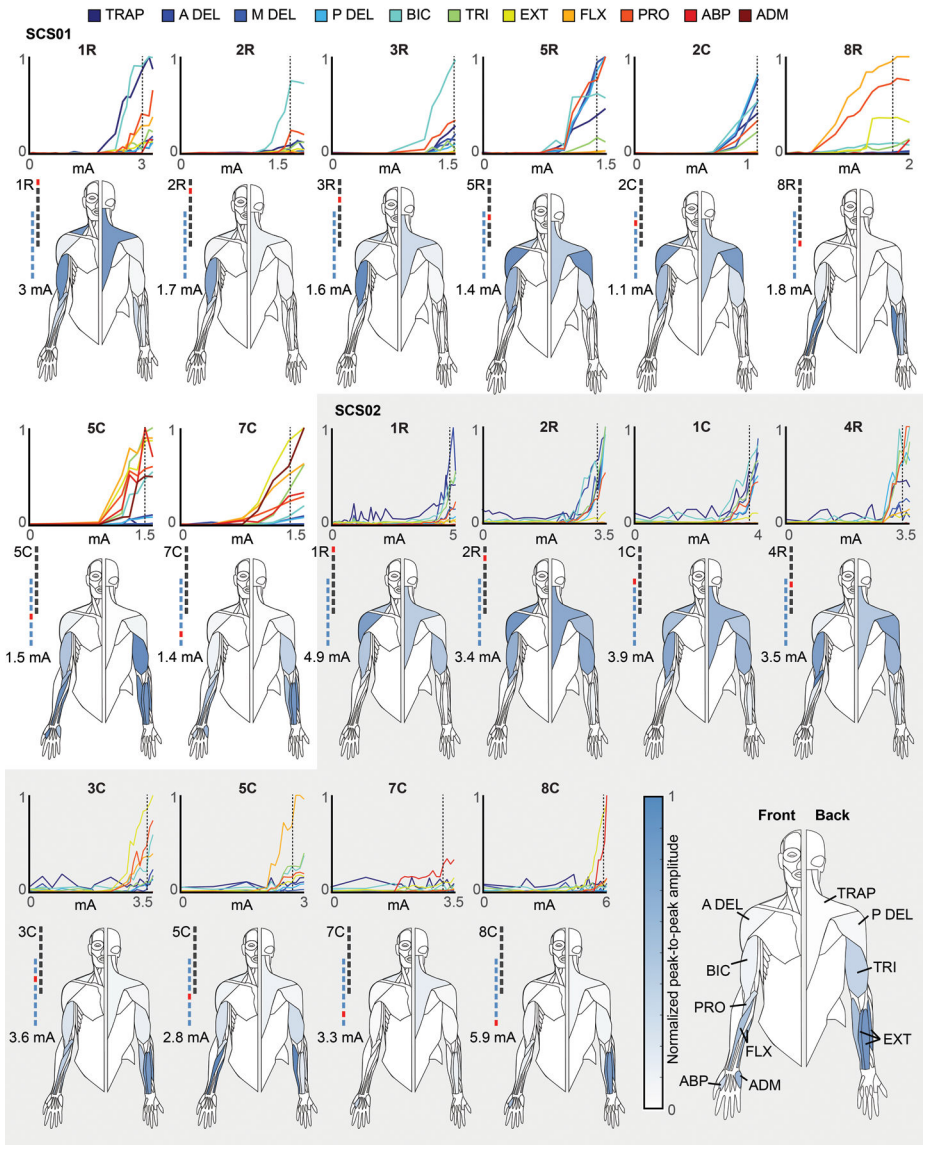

Extended Data Figure 3 |. Muscle recruitment curves.

In each panel we show the recruitment curves obtained with stimulation at 1 Hz at increasing current amplitude for 11 arm and hand muscles: TRAP: trapezius, A, P, M DEL: anterior, posterior and medial deltoid respectively, BIC: biceps, TRI: triceps, EXT: Extensor carpi, FLX: flexor carpi, PRO: pronator teres, ABP: abductor pollicis and ADM: abductor digiti minimi. Below each set of recruitment curves we report the graphical representation of the muscle activation obtained at the amplitude indicated on the left of each human figurine. Interpretation of human figurines is reported in the bottom right. Each muscle is colored with a color scale (on the left) representing the normalized peak-to-peak amplitude of EMG reflex responses obtained at the stimulation amplitude indicated on the left. Peak-to-peak values for each muscle are normalized to the maximum value obtained for that muscle across all contacts and all current amplitudes.

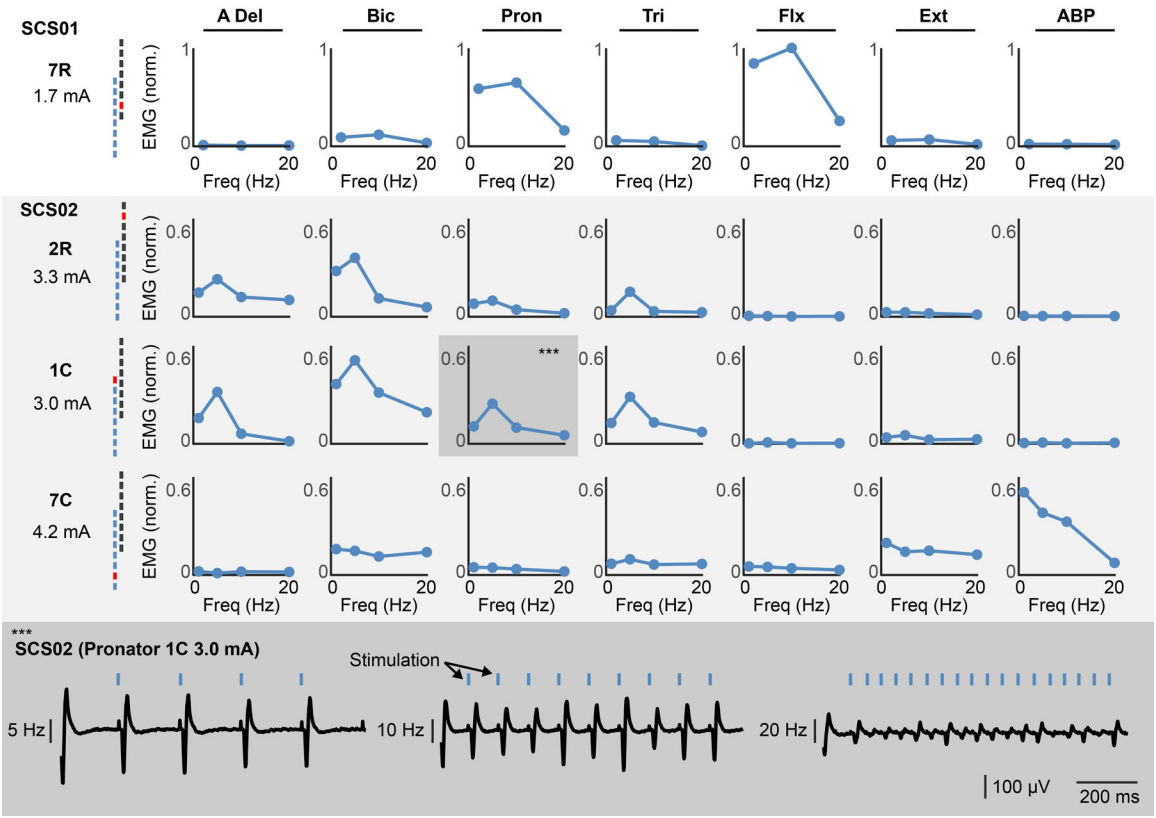

Extended Data Figure 4 |. Frequency dependent suppression.

To demonstrate that SCS recruits arm and hand muscles via direct activation of the primary afferents we performed stimulation at multiple frequencies. The figure reports the spinal reflexes obtained when stimulating at 1, 5, 10 and 20Hz from multiple contacts and multiple muscles. Each plot on the top shows the normalized peak-to-peak reflex amplitude as a function of frequency showing in the muscles that respond to the specific contact substantial frequency dependent suppression at stimulation frequencies greater than 10Hz. On the bottom, we report raw EMG traces that show the classic phenomenon. At 5Hz each pulse of stimulation corresponds to a clear evoked potential in the EMG albeit amplitude slightly diminishes at each pulse. At 10Hz, modulation of peak-to-peak amplitudes becomes more evident, at 20Hz almost complete suppression of EMG evoked responses subsequent to the first is shown. Example is taken from Pronator muscles, contact 1C, (highlighted in darker grey in the top panel).

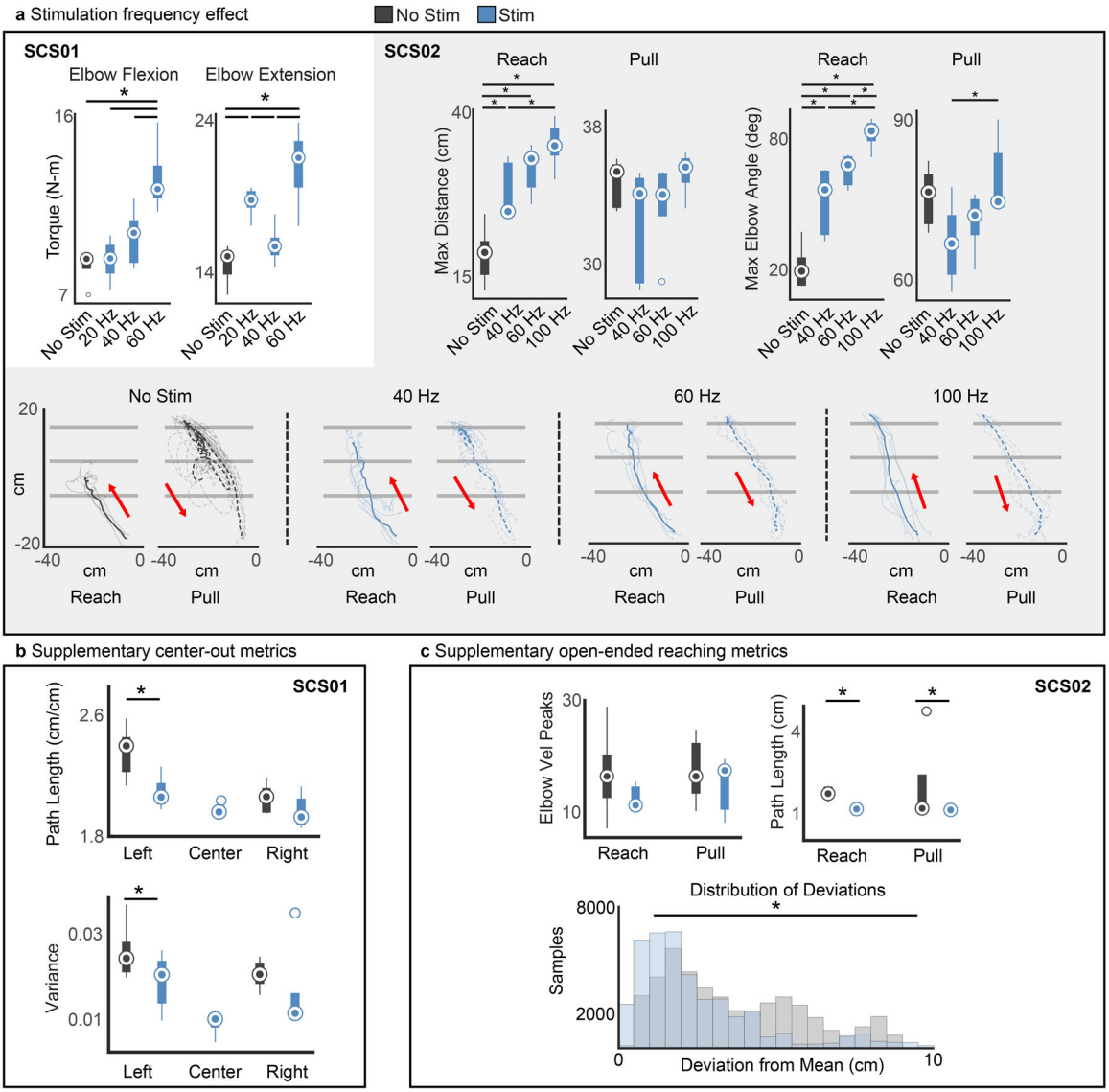

Extended Data Figure 5 |. SCS improves arm kinematics supplementary metrics.

(a) Effect of stimulation frequency shown for SCS01 and SCS02. In SCS01, quantification of isometric torques during single joint flexion and extension is shown for the elbow during no stim (dark grey), 20 Hz (blue), 40 Hz (blue), and 60 Hz (blue). In SCS02, maximum reached distance and elbow angle excursion (max-min) are reported during reach and pull of the reach-out task for no stim (dark grey), 20 Hz (blue), 40 Hz (blue), and 60 Hz (blue). Raw endpoint trajectories for SCS02 are shown in the reach out task during no stim (dark grey), 20 Hz (blue), 40 Hz (blue), and 60 Hz (blue) where SCS02 was tasked to reach beyond the third horizontal line to complete the task. Reach (solid line) and pull (dashed line) trajectories are represented in separate plots. Darker lines represent average trajectories, shaded lines represent single trajectories. **(b)** Quantification of kinematic features for SCS01, path length for completed reach and pull of three targets in cm and variance of the path between trials are reported for no-stim (dark grey) and stim condition (blue). Center target could not be calculated for no-stim condition because

SCS01 did not complete the task. **(c)** Quantification of kinematic features for SCS02, movement smoothness (velocity peaks) and path length in cm for reach and pull separately are reported for no-stim (dark grey) and stim condition (blue). The distribution of deviations from the mean path trajectory is shown in cm (equivalent to variance in SCS01). *Statistics* Distributions of deviations were compared using a two-sample Kolmogorov-Smirnov non-parametric test with alpha=0.05 where p~=0 (where the value was smaller than able to be stored in a double precision variable). All other quantifications are reported using box-plots. For each box, the central circle indicates the median while the bottom and top edges of the box indicate the 25th and 75th percentiles, respectively. The whiskers extend to the minima and maxima data points, not considering outliers. Any outliers are plotted individually with additional circles. Inference on mean differences is performed by bootstrapping the n=5 repetitions obtained for each measurement, with n=10,000 bootstrap samples, and by using a Bonferroni correction when performing multiple comparisons; * indicates statistical significance and rejection of the null hypothesis of no difference with a 95% confidence interval.

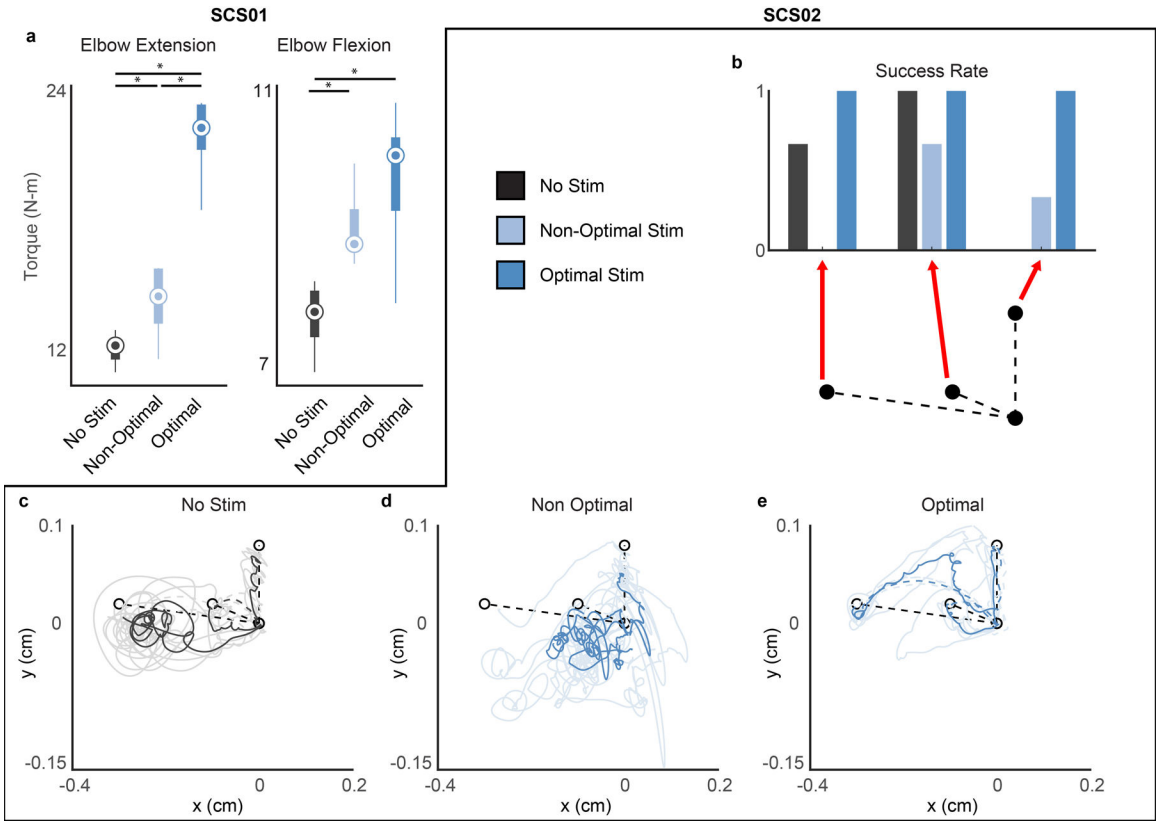

Extended Data Figure 6 |. Optimized SCS leads to best improvement.

(a) Quantification of isometric torques during single joint flexion and extension of the elbow during no stim (dark grey), non-optimal stim (light blue), and optimal stim (blue) for SCS01. **(b)** Quantification of performance for three targets of the center-out task during no stim (dark grey), non-optimal stim (light blue), and optimal stim (blue) normalized from 0 (SCS02 never reached target) and 1 (SCS02 reached target in all trials). n=3 **(c-e)** Raw

endpoint trajectories by SCS02 for three targets of the center-out task during no stim (dark grey), non-optimal stim (light blue), and optimal stim (blue). Darker lines represent average trajectories, shaded lines represent single trajectories. Statistics For quantifications reported using box-plots, the central circle indicates the median while the bottom and top edges of the box indicate the 25th and 75th percentiles, respectively. The whiskers extend to the minima and maxima data points, not considering outliers. Any outliers are plotted individually with additional circles. Inference on mean differences for **(a)** were performed by bootstrapping the n=5 repetitions obtained for each measurement, with n=10,000 bootstrap samples, and by using a Bonferroni correction when performing multiple comparisons; * indicates statistical significance and rejection of the null hypothesis of no difference with a 95% confidence interval.

Extended Data Table 1 | Modified Ashworth Scale longitudinal breakdown.

A breakdown table of the individual MAS scores for each joint tested across all days of the trial. In each case, a score of 0 corresponds to no spasticity, and a score of 4 indicates no mobility at all.

Study Day	Elb Fix	Dig Fix	Shld ER	Shld IR	Shld ABD	FA Sup	Wr Fix	Pron	Elb Ext
SCS01									
1	1.5	1.5	1.5	1.5	1.5	2	-	-	-
2	1.5	1	1.5	1.5	1.5	1.5	-	-	-
3	1.5	1.5	1.5	1.5	1.5	1.5	-	-	-
4	1	1	1.5	1.5	1.5	2	-	-	-
7	1.5	1.5	1.5	1.5	1.5	1.5	-	-	-
8	1	1	1.5	1.5	1	2	-	-	-
9	1	1.5	1.5	1.5	1	2	-	-	-
10	1	1	1	1	1	1.5	-	-	-
11	1	1	1.5	1	1	2	-	-	-
14	1	1	1	1	1.5	1.5	-	-	-
15	1.5	1.5	1.5	1.5	1	2	-	-	-
16	0	1	1.5	1.5	1	1.5	-	-	-
17	1	1.5	1.5	1	1	1.5	-	-	-
18	1	1.5	1	1	1.5	2	-	-	-
22	1	1	1.5	1.5	1.5	1.5	-	-	-
23	1	1.5	1.5	1.5	1.5	2	-	-	-
24	1	1.5	1	1	1	2	-	-	-
Post study 52	1	1.5	1.5	1.5	1	1.5	-	-	-
SCS02									
1	2	1.5	2	0	-	-	3	1.5	-
2	2	1.5	2	1.5	2	-	3	1.5	-
3	2	1.5	2	1	2	-	3	1.5	1.5

Study Day	Elb Fix	Dig Fix	Shld ER	Shld IR	Shld ABD	FA Sup	Wr Fix	Pron	Elb Ext
4	2	1.5	2	1.5	1.5	-	3	2	1
7	2	1.5	2	1	1.5	-	3	1.5	1.5
8	2	2	2	1.5	1.5	-	3	0	0
9	2	2	1.5	0	1.5	-	3	0	0
10	2	1.5	2	1.5	2	-	3	2	1
11	2	2	2	0	1	-	3	1	1
14	2	1	1.5	0	1.5	-	3	0	0
15	2	1.5	2	1.5	1.5	-	3	1	1
16	2	1.5	1.5	1	1.5	-	3	1.5	1
18	2	1.5	2	1.5	2	-	3	2	1
21	1.5	1	1	0	0	-	3	1	0
22	2	1	1.5	0	0	-	3	1	2
23	2	1.5	1.5	1	1.5	-	3	1.5	0
24	2	1.5	2	1	1	-	3	1.5	1

Extended Data Table 2 | Fugl-Meyer Assessment longitudinal breakdown.

A breakdown table of the scores for each of the 7 FM-UE assessment categories. In bold, is the total score for the motor function subcategory which is the sum of the Motor Upper Extremity, Motor Wrist, Motor Hand, and Motor coordination/speed sections. The rightmost column indicates the maximum possible score for each category.

	Pre-Study	Mid Study	End Study	1 mo. Post Study	Total Possible
SCS01					
Passive Joint Motion	21	-	21	21	24
Joint Pain	24	-	24	24	24
Motor Upper extremity	19	20	27	26	36
Motor Wrist	3	3	5	5	10
Motor Hand	9	7	11	11	14
Motor coordination/speed	4	4	4	4	6
Total Motor Function	**35**	**34**	**47**	**46**	**66**
Sensation	11	11	11	11	12
SCS02					
Passive Joint Motion	22	20	20	20	24
Joint Pain	24	23	23	24	24
Motor Upper extremity	11	14	13	12	36
Motor Wrist	0	0	0	0	10
Motor Hand	0	0	1	1	14
Motor coordination/speed	4	4	4	4	6
Total Motor Function	**15**	**18**	**18**	**17**	**66**

	Pre-Study	Mid Study	End Study	1 mo. Post Study	Total Possible
Sensation	2	1	1	2	12

Supplementary Material

Refer to Web version on PubMed Central for supplementary material.

ACKNOWLEDGEMENTS

We thank Jemère Ruby for the design of figure elements in Figure 1, 3 and 4. We wish to thank Tyler Simpson for the engineering support provided. The study was executed through the support of NIH Brain Initiative Grant UG3NS123135–01A1 to MC and DW and internal funding from the Department of Neurological Surgery at the University of Pittsburgh to MC. the Department of Mechanical Engineering and the Neuroscience Institute at Carnegie Mellon University to DW and the Department of Physical Medicine and Rehabilitation at the University of Pittsburgh to EP.

DATA AVAILABILITY

Anonymized data will be uploaded to the Database Archive of the BRAIN Initiative (DABI https://dabi.loni.usc.edu/home). s.

REFERENCES

1. Feigin V, Nguyen G & Roth G Global, Regional, and Country-Specific Lifetime Risks of Stroke, 1990 and 2016. N. Engl. J. Med 379, 2429–2437 (2018). [PubMed: 30575491]
2. Lawrence ES et al. Estimates of the prevalence of acute stroke impairments and disability in a multiethnic population. Stroke 32, 1279–1284 (2001). [PubMed: 11387487]
3. Virani SS et al. Heart Disease and Stroke Statistics—2021 Update: A Report From the American Heart Association. Circulation 143, (2021).
4. Pollock A et al. Interventions for improving upper limb function after stroke. Cochrane Database Syst. Rev (2014) doi:10.1002/14651858.CD010820.pub2.
5. Krakauer JW & Carmichael ST Broken movement: the neurobiology of motor recovery after stroke. (MIT Press, 2017).
6. Hammerbeck U et al. The strength of the corticospinal tract not the reticulospinal tract determines upper-limb impairment level and capacity for skill-acquisition in the sub-acute post-stroke period. Neurorehabil. Neural Repair 35, 812–822 (2021). [PubMed: 34219510]
7. Rosso C et al. Contribution of Corticospinal Tract and Functional Connectivity in Hand Motor Impairment after Stroke. PLOS ONE 8, e73164 (2013). [PubMed: 24086272]
8. Gaunt RA, Prochazka A, Mushahwar VK, Guevremont L & Ellaway PH Intraspinal microstimulation excites multisegmental sensory afferents at lower stimulus levels than local α-motoneuron responses. J. Neurophysiol 96, 2995–3005 (2006). [PubMed: 16943320]
9. Ayers CA, Fisher LE, Gaunt RA & Weber DJ Microstimulation of the lumbar DRG recruits primary afferent neurons in localized regions of lower limb. J. Neurophysiol 116, 51–60 (2016). [PubMed: 27052583]
10. Sharpe AN & Jackson A Upper-limb muscle responses to epidural, subdural and intraspinal stimulation of the cervical spinal cord. J Neural Eng 11, 016005 (2014). [PubMed: 24654267]
11. Sherrington C Flexion-reflex of the limb, crossed extension reflex, and reflex stepping and standing. J Physiol Lond 40, 28–121 (1910). [PubMed: 16993027]
12. Zimmermann JB, Seki K & Jackson A Reanimating the arm and hand with intraspinal microstimulation. J. Neural Eng 8, 054001 (2011). [PubMed: 21828907]

13. Nishimura Y, Perlmutter SI & Fetz EE Restoration of upper limb movement via artificial corticospinal and musculospinal connections in a monkey with spinal cord injury. Front Neural Circuits 7, 57 (2013). [PubMed: 23596396]
14. Shanechi MM, Hu RC & Williams ZM A cortical-spinal prosthesis for targeted limb movement in paralysed primate avatars. Nat Commun 5, 3237 (2014). [PubMed: 24549394]
15. Barra B et al. Epidural electrical stimulation of the cervical dorsal roots restores voluntary upper limb control in paralyzed monkeys. Nat. Neurosci 1–11 (2022). [PubMed: 34992291]
16. Greiner N et al. Recruitment of Upper-Limb Motoneurons with Epidural Electrical Stimulation of the Primate Cervical Spinal Cord. Nat. Commun 12, (2021).
17. Capogrosso M et al. A computational model for epidural electrical stimulation of spinal sensorimotor circuits. J Neurosci 33, 19326–40 (2013). [PubMed: 24305828]
18. Rattay F, Minassian K & Dimitrijevic MR Epidural electrical stimulation of posterior structures of the human lumbosacral cord: 2. quantitative analysis by computer modeling. Spinal Cord 38, 473–489 (2000). [PubMed: 10962608]
19. Harkema S et al. Effect of epidural stimulation of the lumbosacral spinal cord on voluntary movement, standing, and assisted stepping after motor complete paraplegia: a case study. Lancet 377, 1938–47 (2011). [PubMed: 21601270]
20. Angeli CA, Edgerton VR, Gerasimenko YP & Harkema SJ Altering spinal cord excitability enables voluntary movements after chronic complete paralysis in humans. Brain 137, 1394–1409 (2014). [PubMed: 24713270]
21. Angeli CA et al. Recovery of Over-Ground Walking after Chronic Motor Complete Spinal Cord Injury. N Engl J Med 379, 1244–1250 (2018). [PubMed: 30247091]
22. Wagner FB et al. Targeted neurotechnology restores walking in humans with spinal cord injury. Nature 563, 65 (2018). [PubMed: 30382197]
23. Gill ML et al. Neuromodulation of lumbosacral spinal networks enables independent stepping after complete paraplegia. Nat Med 24, 1677–1682 (2018). [PubMed: 30250140]
24. Barolat-Romana G, Myklebust JB, Hemmy DC, Myklebust B & Wenninger W Immediate effects of spinal cord stimulation in spinal spasticity. J. Neurosurg 62, 558–562 (1985). [PubMed: 3871847]
25. Carhart MR, He J, Herman R, D'Luzansky S & Willis WT Epidural spinal-cord stimulation facilitates recovery of functional walking following incomplete spinal-cord injury. IEEE Trans Neural Syst Rehabil Eng 12, 32–42 (2004). [PubMed: 15068185]
26. Danner SM et al. Human spinal locomotor control is based on flexibly organized burst generators. Brain 138, 577–88 (2015). [PubMed: 25582580]
27. Ajiboye AB et al. Restoration of reaching and grasping movements through brain-controlled muscle stimulation in a person with tetraplegia: a proof-of-concept demonstration. The Lancet (2017) doi:10.1016/S0140-6736(17)30601-3.
28. Biasiucci A et al. Brain-actuated functional electrical stimulation elicits lasting arm motor recovery after stroke. Nat. Commun 9, 1–13 (2018). [PubMed: 29317637]
29. Moraud EM et al. Mechanisms Underlying the Neuromodulation of Spinal Circuits for Correcting Gait and Balance Deficits after Spinal Cord Injury. Neuron 89, 814–28 (2016). [PubMed: 26853304]
30. Capogrosso M et al. A brain-spine interface alleviating gait deficits after spinal cord injury in primates. Nature 539, 284–288 (2016). [PubMed: 27830790]
31. Guiho T, Baker SN & Jackson A Epidural and transcutaneous spinal cord stimulation facilitates descending inputs to upper-limb motoneurons in monkeys. J. Neural Eng 18, 046011 (2021).
32. Kato K, Nishihara Y & Nishimura Y Stimulus outputs induced by subdural electrodes on the cervical spinal cord in monkeys. J. Neural Eng 17, 016044 (2020). [PubMed: 32023224]
33. Alam M et al. Evaluation of optimal electrode configurations for epidural spinal cord stimulation in cervical spinal cord injured rats. J. Neurosci. Methods 247, 50–57 (2015). [PubMed: 25791014]
34. Lu DC et al. Engaging Cervical Spinal Cord Networks to Reenable Volitional Control of Hand Function in Tetraplegic Patients. Neurorehabil Neural Repair 30, 951–962 (2016). [PubMed: 27198185]

35. Lemon RN Descending pathways in motor control. Annu Rev Neurosci 31, 195–218 (2008). [PubMed: 18558853]
36. Kiehn O Decoding the organization of spinal circuits that control locomotion. Nat Rev Neurosci 17, 224–38 (2016). [PubMed: 26935168]
37. Kofler M, Quirbach E, Schauer R, Singer M & Saltuari L Limitations of intrathecal baclofen for spastic hemiparesis following stroke. Neurorehabil. Neural Repair 23, 26–31 (2009). [PubMed: 18796543]
38. Chandrasekaran S et al. Sensory restoration by epidural stimulation of the lateral spinal cord in upper-limb amputees. Elife 9, e54349 (2020). [PubMed: 32691733]
39. Holsheimer J Which Neuronal Elements are Activated Directly by Spinal Cord Stimulation. Neuromodulation Technol. Neural Interface 5, 25–31 (2002).
40. Schirmer CM et al. Heuristic map of myotomal innervation in humans using direct intraoperative nerve root stimulation. J Neurosurg Spine 15, 64–70 (2011). [PubMed: 21476796]
41. Scott SH Apparatus for measuring and perturbing shoulder and elbow joint positions and torques during reaching. J. Neurosci. Methods 89, 119–127 (1999). [PubMed: 10491942]
42. Lyle RC A performance test for assessment of upper limb function in physical rehabilitation treatment and research. Int. J. Rehabil. Res 4, 483–492 (1981). [PubMed: 7333761]
43. Waltz JM, Reynolds LO & Riklan M Multi-lead spinal cord stimulation for control of motor disorders. Stereotact. Funct. Neurosurg 44, 244–257 (1981).
44. Cioni B, Meglio M, Prezioso A, Talamonti G & Tirendi M Spinal cord stimulation (SCS) in spastic hemiparesis. Pacing Clin. Electrophysiol. PACE 12, 739–742 (1989). [PubMed: 2470060]
45. Pirondini E et al. Poststroke arm and hand paresis: should we target the cervical spinal cord? Trends Neurosci. (2022).
46. Inanici F, Brighton LN, Samejima S, Hofstetter CP & Moritz CT Transcutaneous spinal cord stimulation restores hand and arm function after spinal cord injury. IEEE Trans Neural Syst Rehabil Eng 29, 310–319 (2021). [PubMed: 33400652]
47. Capogrosso M et al. Configuration of electrical spinal cord stimulation through real-time processing of gait kinematics. Nat Protoc (2018) doi:10.1038/s41596-018-0030-9.
48. de Freitas RM et al. Selectivity and excitability of upper-limb muscle activation during cervical transcutaneous spinal cord stimulation in humans. J. Appl. Physiol (2021).
49. Colombo EV et al. Epidural spinal cord stimulation for neuropathic pain: a neurosurgical multicentric Italian data collection and analysis. Acta Neurochir. (Wien) 157, 711–720 (2015). [PubMed: 25646850]
50. Corbetta D, Sirtori V, Castellini G, Moja L & Gatti R Constraint-induced movement therapy for upper extremities in people with stroke. Cochrane Database Syst. Rev (2015) doi:10.1002/14651858.CD004433.pub3.
51. French B et al. Repetitive task training for improving functional ability after stroke. Cochrane Database Syst. Rev (2016) doi:10.1002/14651858.CD006073.pub3.
52. Rowald A et al. Activity-dependent spinal cord neuromodulation rapidly restores trunk and leg motor functions after complete paralysis. Nat. Med 28, 260–271 (2022). [PubMed: 35132264]
53. Krakauer JW & Cortés JC A non-task-oriented approach based on high-dose playful movement exploration for rehabilitation of the upper limb early after stroke: a proposal. NeuroRehabilitation 43, 31–40 (2018). [PubMed: 30056438]
54. Reinkensmeyer DJ, Emken JL & Cramer SC Robotics, motor learning, and neurologic recovery. Annu Rev Biomed Eng 6, 497–525 (2004). [PubMed: 15255778]
55. Yeh F-C et al. Population-averaged atlas of the macroscale human structural connectome and its network topology. NeuroImage 178, 57–68 (2018). [PubMed: 29758339]
56. Yeh F-C & Tseng W-YI NTU-90: A high angular resolution brain atlas constructed by q-space diffeomorphic reconstruction. NeuroImage 58, 91–99 (2011). [PubMed: 21704171]
57. Yeh F-C, Wedeen VJ & Tseng W-YI Generalized $ q$-Sampling Imaging. IEEE Trans. Med. Imaging 29, 1626–1635 (2010). [PubMed: 20304721]
58. Yeh F-C, Liu L, Hitchens TK & Wu YL Mapping immune cell infiltration using restricted diffusion MRI. Magn. Reson. Med 77, 603–612 (2017). [PubMed: 26843524]

59. Yeh F-C, Verstynen TD, Wang Y, Fernández-Miranda JC & Tseng W-YI Deterministic Diffusion Fiber Tracking Improved by Quantitative Anisotropy. PLOS ONE 8, e80713 (2013). [PubMed: 24348913]

60. Yeh F-C et al. Automatic Removal of False Connections in Diffusion MRI Tractography Using Topology-Informed Pruning (TIP). Neurotherapeutics 16, 52–58 (2019). [PubMed: 30218214]

61. Fugl-Meyer AR, Jääskö L, Leyman I, Olsson S & Steglind S A method for evaluation of physical performance. Scand J Rehabil Med 7, 13–31 (1975). [PubMed: 1135616]

62. Yozbatiran N, Der-Yeghiaian L & Cramer SC A standardized approach to performing the action research arm test. Neurorehabil. Neural Repair 22, 78–90 (2008). [PubMed: 17704352]

63. Israely S, Leisman G, Machluf CC & Carmeli E Muscle Synergies Control during Hand-Reaching Tasks in Multiple Directions Post-stroke. Front. Comput. Neurosci 12, (2018).

64. Turpin NA, Uriac S & Dalleau G How to improve the muscle synergy analysis methodology? Eur. J. Appl. Physiol 121, 1009–1025 (2021). [PubMed: 33496848]

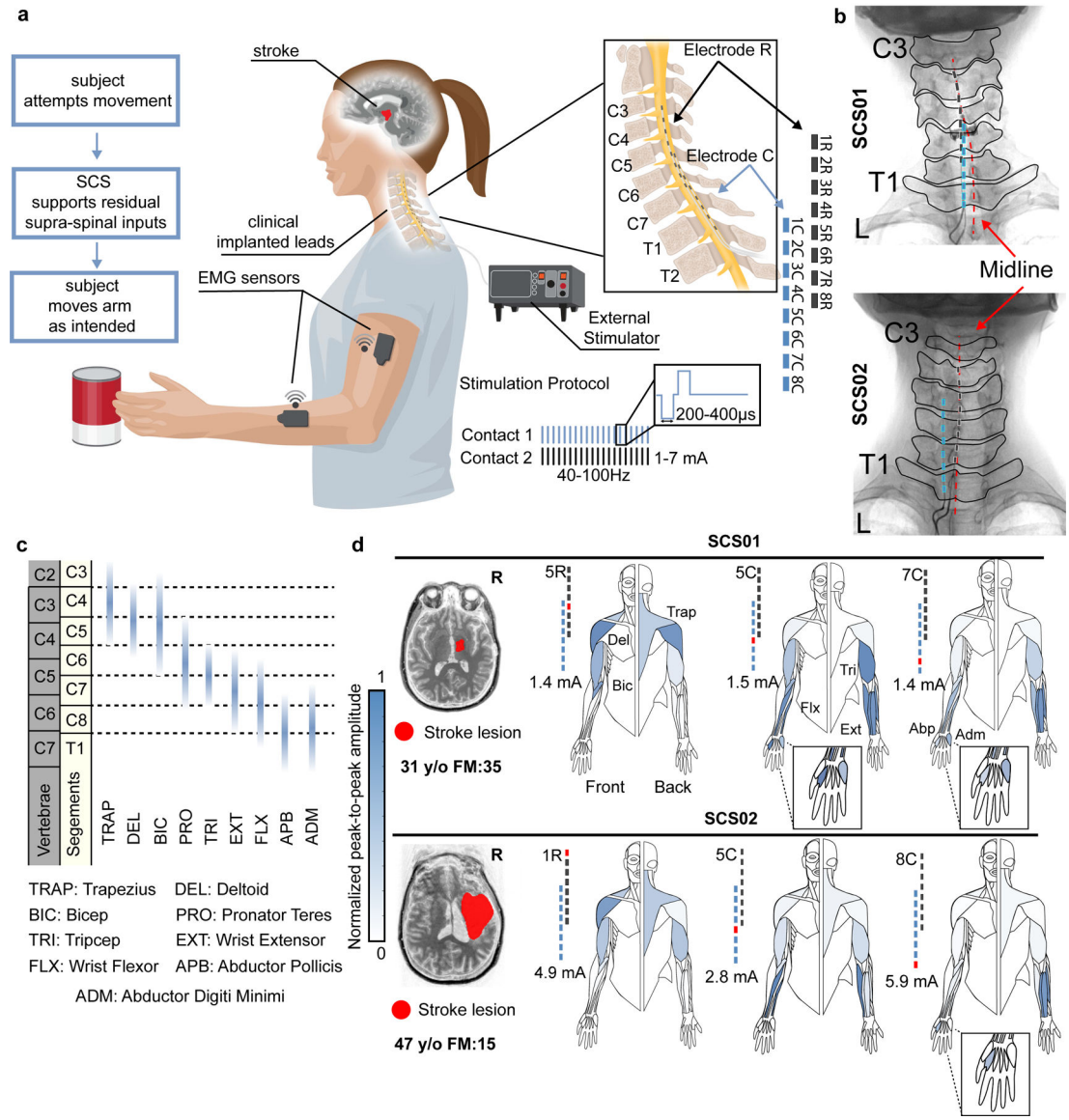

Figure 1 |. Experimental set-up and stimulation arrangement.

(a) Schematic of the experimental apparatus and paradigm. While participants performed an upper limb motor task, we measured wireless electromyographic (EMG) activity from muscles of the arm and hand. We delivered electrical stimulation to the cervical spinal cord via two 8-contact leads (Rostral, R; Caudal, C) implanted in the cervical spinal cord. Simultaneous stimulation through selected contacts was controlled via percutaneous connections using an external stimulator. (b) X-rays of both participants showing the location of the contacts of the Rostral (blue) and Caudal (dark grey) leads with respect to the midline (in dashed red). (c) Location of the motoneurons of arm and hand muscles in the human spinal cord in relation to spinal segments (light yellow) and vertebrae (grey). We estimated the rostro-caudal position of motoneuron pools (blue) from Schirmer 2011. (d) Graphical representation of muscle activation obtained by stimulating through selected contacts (labeled in red on the left of each human figurine). Each human figurine represents

the front view (left half) and back view (right half) of arm muscles (See also Extended Data Figure 3). Each muscle is colored with a color scale (on the left) representing the normalized peak-to-peak amplitude of EMG reflex responses obtained during 1 Hz stimulation at the stimulation amplitude indicated on the left. Peak-to-peak values for each muscle are normalized to the maximum value obtained for that muscle across all contacts and all current amplitudes. On the left, MRI of each participant is shown with segmented lesion in red.

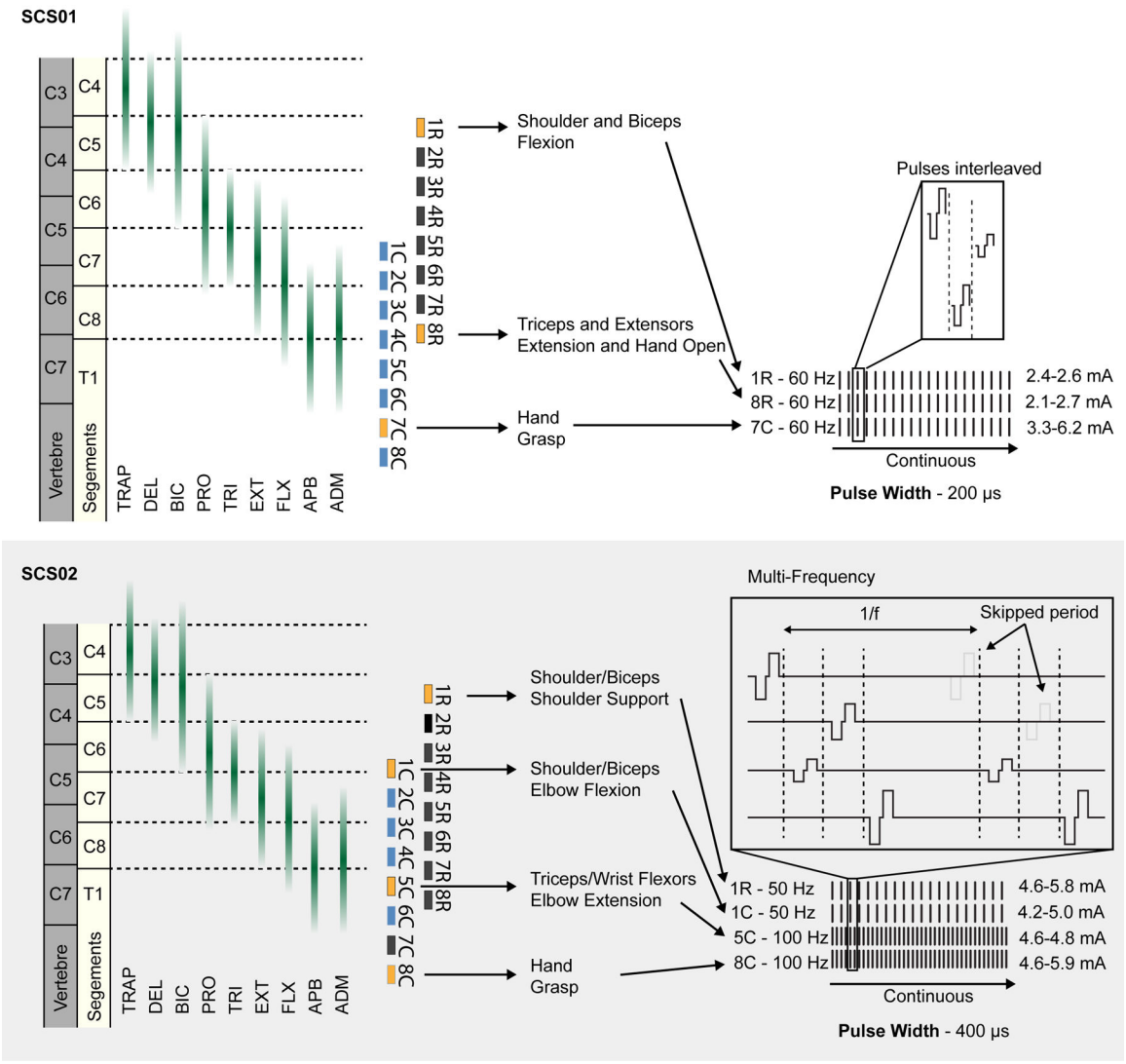

Figure 2 |. Optimized continuous stimulation protocols.

Stimulation protocol used to achieve maximum assistive benefit for SCS01 **(top)** and SCS02 **(bottom). (top)** For SCS01, contacts 1R and 8R on the rostral lead and 7C on the caudal lead were simultaneously and continuously activated at a fixed 60 Hz frequency and 200 μs pulse width. These electrodes corresponded shoulders and biceps (1R); triceps, extensors, and hand opening (8R); and hand grasp (7C). Amplitudes were changed daily based on participant preference and were set to 2.4–2.6 mA (1R), 2.1–2.7 mA (8R), and 3.3–6.2 mA (7C). **(bottom)** For SCS02, contacts 1R on the rostral lead, and 1C, 5C, and 8C on the caudal lead were simultaneously and continuously stimulated. These electrodes corresponded to muscles related to shoulder support (1R); elbow flexion (1C); elbow extension and wrist flexion (5C); and hand grasp (8C). Contacts 1R and 1C were stimulated at 50 Hz while 5C and 8C were stimulated at 100 Hz all at a fixed pulse width of 400 μs. A reduced frequency was used on contacts corresponding to elbow flexion to bias the assistive benefit of stimulation toward elbow extension. Multi-frequency stimulation was achieved by skipping every other period of a 100 Hz stimulation protocol on channels stimulating

at 50 Hz. Location of the motoneurons of arm and hand muscles in the human spinal cord in relation to spinal segments (light yellow) and vertebrae (grey) is shown on the left for SCS01 and SCS02. We estimated the rostro-caudal position of motoneuron pools (green) from Schirmer 2011.

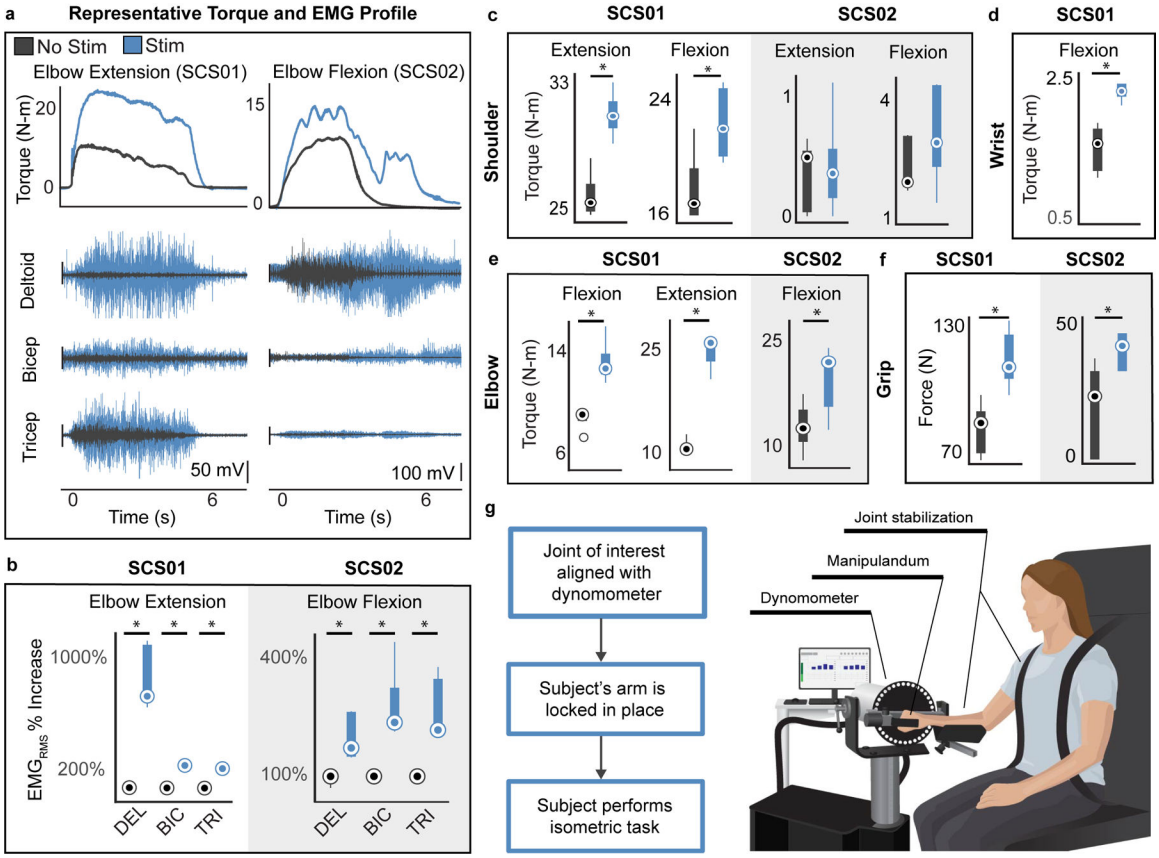

Figure 3 |. SCS immediately improved strength.

(a) examples of single synchronized raw traces for torques and EMGs signals during isometric maximum voluntary contractions for extension (SCS01, left) and flexion (SCS02, right) of the elbow in the HUMAC NORM (see panel **g**). **(b)** quantification of the root mean square value of EMG traces with and without stimulation during isometric elbow extension (SCS01) and flexion (SCS02) **(c, d, e)** quantification of isometric torques during single joint flexion and extension for SCS01 and SCS02 at shoulder, elbow and wrist **(f)** quantification of isometric grip-strength measured with a hand-held dynamometer with and without stimulation. **(g)** schematic of the isometric torque test (wrist configuration in the example) in the HUMAC NORM. *Statistics* all quantifications are reported using box-plots. For each box, the central circle indicates the median while the bottom and top edges of the box indicate the 25th and 75th percentiles, respectively. The whiskers extend to the minima and maxima data points, not considering outliers. Any outliers are plotted individually with additional circles. Inference on mean differences is performed by bootstrapping the n=5 repetitions obtained for each measurement, with n=10,000 bootstrap samples; * indicates statistical significance and rejection of the null hypothesis of no difference with a 95% confidence interval.

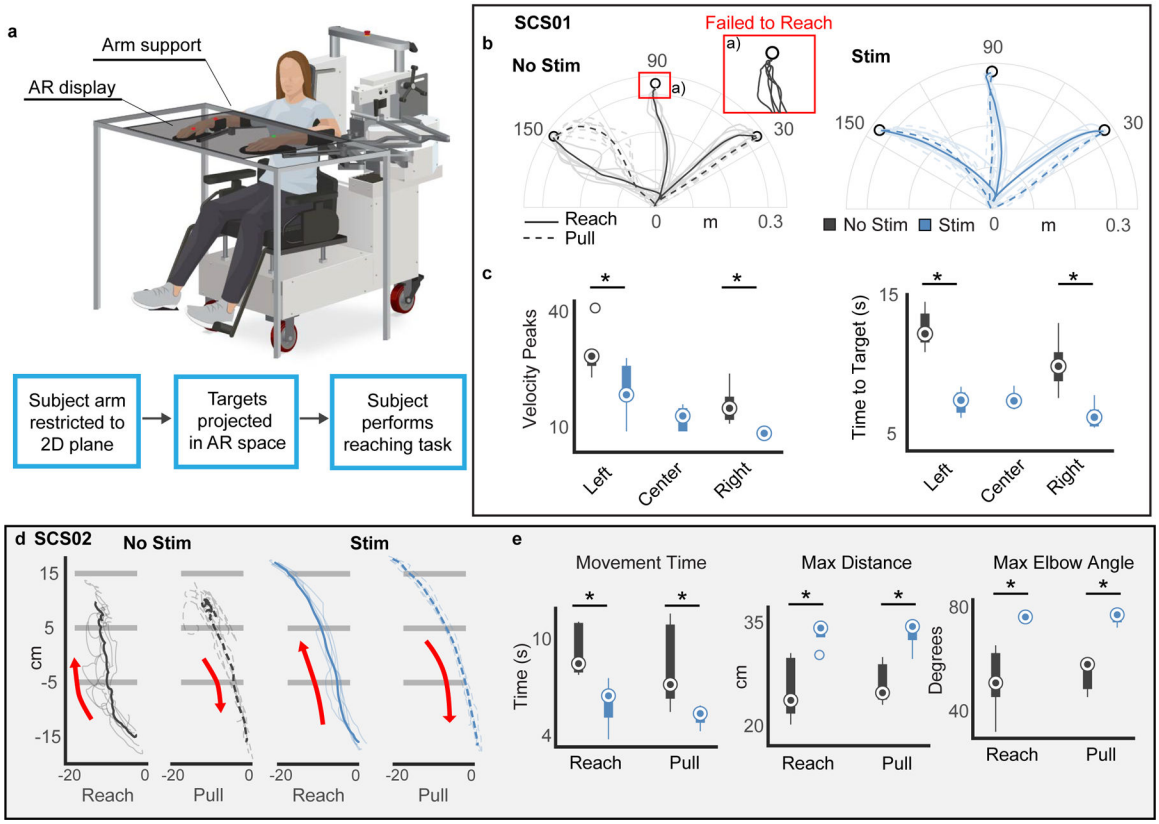

Figure 4 |. SCS immediately improves arm kinematics.

(a) schematic of the experimental set-up for planar reach out tasks using the KINARM. **(b)** Examples of raw endpoint trajectories for SCS01 in the reach out task without stimulation (dark grey,left) and with stimulation (blue, right). Inset shows inability to reach central target without stimulation. Solid lines are reach trajectories and dashed lines represent pull trajectories. Darker lines represent average trajectories, shaded lines represent individual trajectories. **(c)** Quantification of kinematic features, movement smoothness (velocity peaks) and time to reach target in seconds. Center target could not be calculated for no-stim condition because SCS01 did not complete the task. **(d)** Examples of raw endpoint trajectories for SCS02 in the reach out task. SCS02 was tasked to reach beyond the third horizontal line to complete the task. Reach (solid line) and pull (dashed line) trajectories are represented in separate plots. Darker lines represent average trajectories, shaded lines represent individual trajectories. **(e)** Quantification of kinematic features for SCS02, Reach time (equivalent to time to target in SCS01), Maximum reached distance and elbow angle excursion (max-min) are reported for no-stim (dark grey) and stim condition (blue). *Statistics* all quantifications are reported using box-plots. For each box, the central circle indicates the median while the bottom and top edges of the box indicate the 25th and 75th percentiles, respectively. The whiskers extend to the minima and maxima data points, not considering outliers. Any outliers are plotted individually with additional circles. Inference on mean differences is performed by bootstrapping the n=6 (center out) or n=5 (open-ended reaching) repetitions obtained for each measurement, with n=10,000 bootstrap samples; *

indicates statistical significance and rejection of the null hypothesis of no difference with a 95% confidence interval.

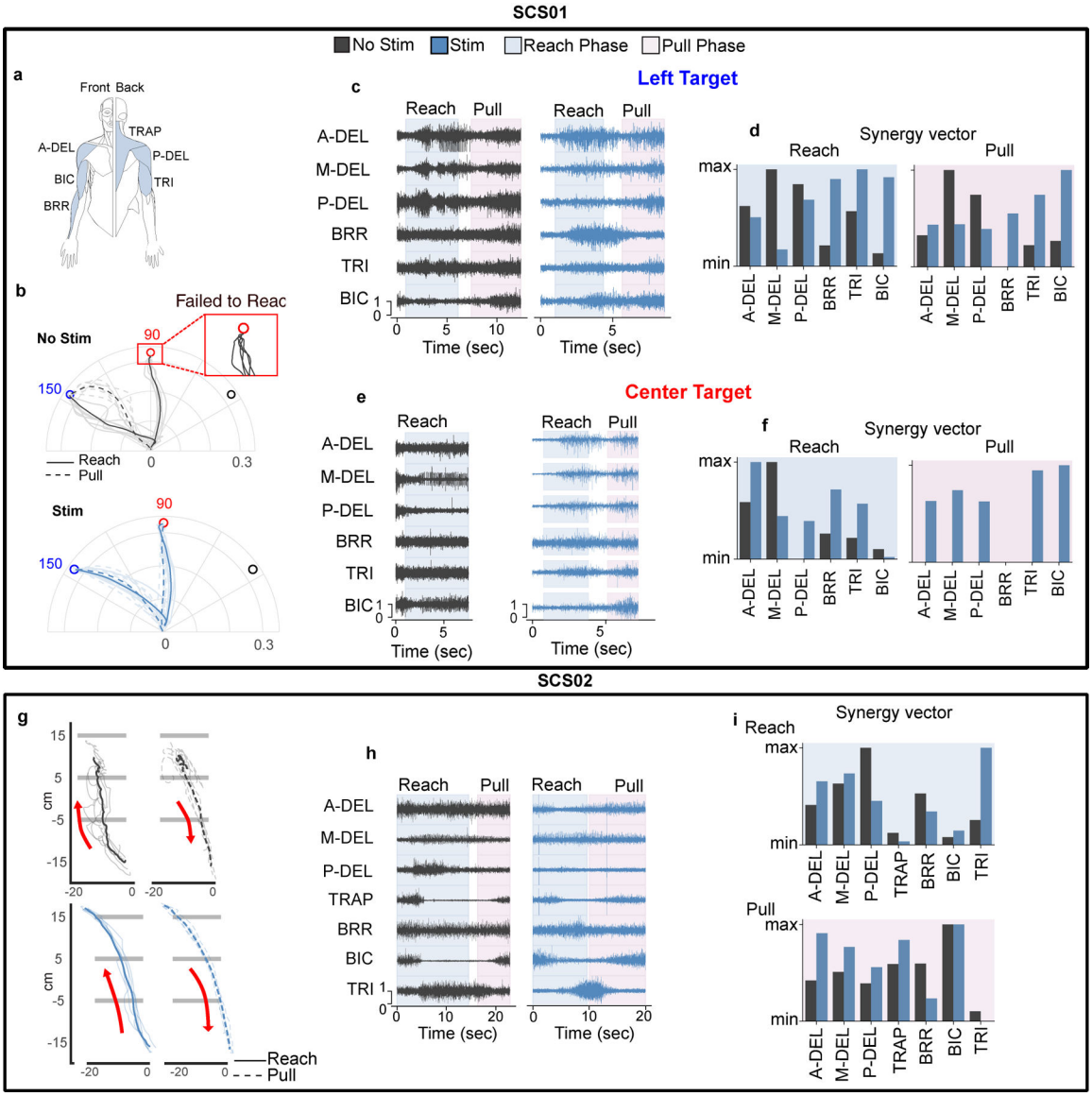

Figure 5 |. Muscle activation pattern during planar movement.

a) Muscle label abbreviation used in the figure. Respective muscles are highlighted in light blue. **(b)** Kinematic trajectories during planar center-out task for two different targets (left and center) for stimulation off (dark grey) and on (blue) conditions. The inset block shows the inability of SCS01 to reach to the center target without stimulation. Solid lines are reach trajectories and dashed lines represent pull trajectories. Darker lines represent average trajectories, shaded lines represent single trajectories. **(c) Normalized** EMG signals for the left target during reach (light blue highlight) and pull phase (pink highlight) without stimulation (dark grey) and with stimulation (blue). **(d)** synergy vector for the left target corresponding to the increasing time-series synergy activation. **(e) Normalized** EMG signals for the center target during reach (light blue highlight) and pull phase (pink highlight) without stimulation (dark grey) and with stimulation (blue). **(f)** Synergy vector for the center target with stimulation (blue) and without stimulation (dark grey) for reach (light

blue highlight) and pull phase (pink highlight). **(g)** Kinematic trajectories for reaching-out task with stimulation (blue) and without stimulation (dark grey) for reach (solid line) and pull phase (dashed line) for SCS02. Darker lines represent average trajectories, shaded lines represent single trajectories. **(h) Normalized EMG signals** with stimulation (blue) and without stimulation (dark grey) during reach (blue highlight) and pull phase (pink highlight) for planar reaching-out task. **(i)** Synergy vector corresponding to the reach (blue highlight) and pull phase (pink highlight) of the movement with stimulation (blue) and without stimulation (dark grey).

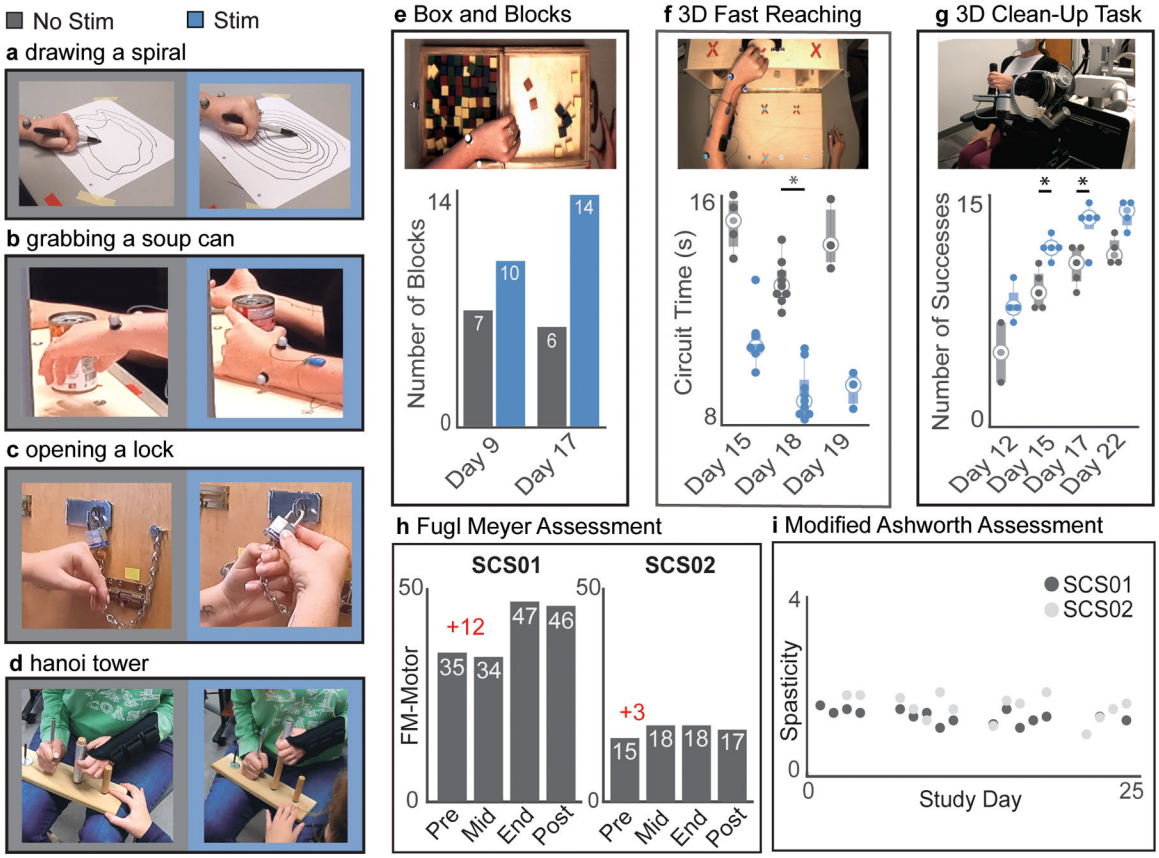

Figure 6 |. SCS improves function.

(a,b,c) frame captures from videos showing improved functional abilities of different simulated activities of daily living: drawing a spiral, reaching and grasping a soup can, opening a lock for SCS01. Left no stimulation, right with stimulation. (d) picture report frames from video of SCS02 performing a modified “Hanoi tower” task in which she was tasked to move a hollow cylinder from a base pole to another. Left no stimulation, right with stimulation. (e,f) representative pictures and quantification of task performances for SCS01 box and blocks and 3D fast reaching tasks performed on multiple days. Individual data points are also shown as some datasets contain less than 5 data points. (g) picture of the 3D reaching task using the Armeo Power for SCS02 and relative task performance on multiple days. Individual data points are also shown as some datasets contain less than 5 data points. (h) Fugl-Meyer assessment at different time points for SCS01 and SCS02 including 4-weeks post-study. (i) normalized spasticity level obtained by averaging Modified Ashworth Score at each joint for SCS01 (dark grey) and SCS02 (light grey). *Statistics* all quantifications are reported using box-plots. For each box, the central circle indicates the median while the bottom and top edges of the box indicate the 25th and 75th percentiles, respectively. The whiskers extend to the minima and maxima data points, not considering outliers. Any outliers are plotted individually with additional circles. For datasets containing 5 or more data points, inference on mean differences is performed by bootstrapping n=5 to 9 repetitions obtained for each measurement, with n=10,000 bootstrap samples; * indicates

statistical significance and rejection of the null hypothesis of no difference with a 95% confidence interval.

Video 1:

Video 2:

Video 3:

Video 4:

Video 5: